Expertise
and insight
for the future

Nargiza Deidieva

Software Design for Head Impact Assessment Device Prototype in Contact Sports

Metropolia University of Applied Sciences

Bachelor of Engineering

Degree Programme in Electronics Engineering

Bachelor’s Thesis

27 May 2020

metropolia.fi/en

Metropolia
University of Applied Sciences

Author Title Number of Pages Date	Nargiza Deidieva Software Design for Head Impact Assessment device prototype in Contact Sports 49 pages 27 May 2020
Degree	Bachelor of Engineering
Degree Programme	Electronics Engineering degree programme
Professional Major	Electronics
Instructors	Iiro Virtanen, Chief Operating Officer (MDS Finland) Matti Fischer, Principal Lecturer (Metropolia UAS)

Head impacts in contact sports are responsible for concussions in contact sports athletes. A concussion is a head injury affecting the brain physiology caused by the destruction of neural tissue. Concussions are often underreported by contact sport athletes or undiagnosed by medical professionals. To improve athletes' well-being, the head impact severity measurement device prototype was designed. The goal of this thesis work was to design a software part of the device prototype that would be installed on a helmet, to collect and measure the magnitudes of head impacts that may cause concussion in real-time and send the obtained data over BLE to the mobile phone. The obtained information will be used by medical professionals for monitoring and assessing the head impact magnitudes.

The measurement variables for the device prototype were linear acceleration and rotational velocity. The device prototype development included defining the requirements, design planning, development, and testing. Head impact telemetry system regulations for helmeted devices, general requirements for wearable devices defined the requirements for the device prototype. The design phase performed a comparison of tools and devices in accordance with the requirements. During the development phase the embedded software system was implemented.

Testing was performed by applying linear acceleration and rotational velocity forces. The results matched the expected results that were set by datasheets for every breakout board in the device prototype. The device prototype was successfully developed and has passed all the tests.

Keywords	Head impact measurement software, HITS device, Concussion, Bluetooth Low Energy, Internet of things, ARM processor

Contents

List of Abbreviations

ACK	Acknowledge
ARM	Advanced RISC (Reduced Instruction Set Computer) Machines
ARM M4	Advanced RISC (Reduced Instruction Set Computer) Machines Microcontroller 4th edition
ATT	Attribute Protocol
BLE	Bluetooth Low Energy
BOM	Bill of Material
BT SIG	Bluetooth Special Interest Group
BW	Bandwidth
CT scan	Computer Tomography scan
GATT	Generic Attribute Profile
GCC	GNU (GNU is not Unix) Compiler Collection
EEPROM	Electrically Erasable Programmable Read-Only Memory
HITS	Head Impact Telemetry System
IDE	Integrated Development Environment
IIC or I2C	Inter-Integrated Circuit
IRK	Identity Resolving Key
MAC	Media Access Control Address

MEMS	Micro-ElectroMechanical Systems
MRI	Magnetic Resonance Imaging
NACK	Not Acknowledge
OS	Operating System
PCB	Printed Circuit Board
SPI	Serial Peripheral Interface
TBI	Traumatic Brain Injury
UART	Universal Asynchronous Receiver-Transmitter
USB	Universal Serial Bus
UUID	Universally Unique Identifier
ZRO	Zero-Rate Output

1 Introduction

Concussion is a common injury among contact sports players that usually comes from hitting to a head and jerking of the head. It is often difficult for health professionals to diagnose head injuries because brain imaging devices cannot detect most head injuries. Moreover, there is a common misconception that in order to get a concussion it is necessary to lose consciousness, but the loss consciousness precedes concussion in only 10 percent of cases [1]. Such misconception makes contact sport athletes to overlook other more subtle concussion symptoms. In many cases, it is important to diagnose concussion in the early stages, because in most cases, immediate treatment guarantees a decrease in the magnitude of the development of a head injury, since brain injury develops gradually days after the head impact incident.

One of the most popular sports in Finland is hockey, and hockey is one of the contact sports with the largest number of concussion cases is recorded. To increase the safety of hockey players, early diagnosis of concussion, and establishing the degree of an injury to the head of hockey players were necessary. The goal of this thesis work was to develop a prototype device for collecting and quantifying the impact forces to the athletes' heads. The process of this thesis work included designing a software system of the device prototype, device prototype development, testing, and presentation of the results.

The device was to be installed on the helmet of a sports player and collect data on head impacts during games and trainings. A device for collecting data on head impacts consisted of hardware and software elements. This thesis work describes the software system development process. The device was to classify head impacts according to linear acceleration and rotation speed. These data can be further used by medical professionals to determine the severity of a head injury.

MDS Finland employees were managing and guiding the development of the device prototype. The device prototype is a property of MDS Finland company.

The practical significance of the device is the use of the developed prototype of the device to determine the degree of injury to the head (brain) of hockey players. The device will help to diagnose concussions and prevent the effects of injuries in the early stages.

The device will be useful for determining and classifying the degree of severity of a head injury according to linear acceleration and rotational speed.

2 Medical Devices and Services Finland

Medical Devices and Services Finland (or MDS Finland) is a company specializing in medical devices development, quality management and regulatory approvals, and human resources. MDS Finland was founded in 2015. The company is privately held and consists of 2-10 employees. MDS Finland's organization structure is a Horizontal/Flat structure, where employees have superiors, but at the same time are held responsible for their decisions.

MDS Finland's main clients are medical devices start-up companies, hospitals, and individuals. The main products of the company include PCB design and software development for medical devices. MDS provides trainings on quality management, medical device registrations services for start-up companies that deal with medical devices [2.].

3 Theoretical Framework

3.1 Importance of Brain Injuries in Contact Sports

Many contact sports players get injuries that are caused by impact or contact with objects, surfaces, or other people. Such injuries are common in contact sports such as football, ice hockey, motor racing, and skiing. Common contact sports injuries include bruising, head injuries, cuts, muscle pain spinal injuries, fractures and dislocated joints, etc. While many of the injuries can be noticed and treated on time, there are some injuries that are often easy to overlook. It has been difficult to prevent or detect concussions because most of the head injuries cannot be seen on MRI or CT scans [4]. Moreover, repeated concussions could lead an athlete to get chronic traumatic encephalopathy, Alzheimer’s disease, Parkinsonism, and Amyotrophic lateral sclerosis [3.].

Statistics published by the UPMC Sports Medicine Concussion Program state that around 1.7- 3 million contact sports concussions occur every year, 50% of concussions are unreported or undetected. [5.]

Concussions are common injuries in contact sports athletes. If undetected on time concussions cause health complications like chronic traumatic encephalopathy, which leads athletes to premature retirement, premature death, problems with behavior, mood problems, and even suicide [3.].

3.2 Traumatic Brain Injury

Traumatic brain injury (TBI) is damage to the brain induced by a blow or jolt to the head. Common causes include car accidents, falls, contact sports injuries, and assault. TBI ranges from mild concussions to severe irreversible brain damages like CTE. The TBI treatment involves medication for light head injuries and intensive care and surgery in severe cases. Brain injury has lasting effects on an individual’s physical capabilities, mental abilities, emotions and personality. Intensive care for relearning skills, and rehabilitation are often necessary for individuals who have moderate or severe TBI.

TBI appears in mere milliseconds to minutes after an impact to the head, but it does not stop there, it progresses to even more serious injury days after the head impact incident, if not treated on time. The injury that occurs during a head impact is classified as primary injury. Usually primary injuries affect a specific lobe of the brain or the whole brain. In some cases, the skull may be fractured. During the impact of an accident, the brain bounces back and forth inside the skull causing bruising, bleeding, and tearing of brain tissue. Immediate symptoms may be confusion, loss of memory, blurry vision and dizziness, or lose consciousness. Right after the incident the person may seem fine, that is why it is usually very easy to overlook the TBI. Yet, several days after the incident, the person's condition may worsen rapidly. Primary trauma occurs results in a secondary trauma- just like any other bruise, it swells – pressing itself against the skull and reducing the flow of blood. The secondary injury is often more damaging than the primary injury.

Traumatic brain injuries can be categorized according to the degree of severity of injury and mechanism of impact:

- Mild: a person's eyes are open and he or she is conscious. Symptoms may include disorientation, confusion, memory loss, headache, and brief loss of consciousness.

- Moderate: a person's eyes open to stimulation and he or she is lethargic. Symptoms: loss of consciousness lasting between 20 minutes and 6 hours, sleepiness. There is some brain swelling or bleeding, which causes a person to feel sleepiness, but he or she still reacts to stimulation and is rousable.

- Severe: a person is unconscious, even with stimulation. Symptom- loss of consciousness lasting more than 6 hours.

Contact sports plays often include mild TBIs, and rarely moderate TBIs and almost never severe TBIs. Mild TBIs are also known as concussions, that is why this thesis work focused on concussion mechanism and concussion measurement and prevention [6.].

3.3 Concussion

Concussion is a traumatic brain injury of a mild form, that affects one's brain function. Concussion is usually caused by a blow to the head or intense shaking of the head. Concussion changes how the brain functions, hence it is a functional injury. When the body or the head is struck, the brain will bounce around inside the skull which causes in bruising of brain tissue. Concussions in contact sports is an important issue because of its potential threat to the development and functioning of players' brains.

There is a common misconception that one needs to have loss of consciousness in order to be considered to have a concussion, but in sports when one gets a concussion, loss of consciousness only occurs roughly 10 percent of the cases. Sometimes the cause of the concussion might be something small: like an elbow hitting the head or just a tap of somebody coming down from a rebound and hitting you on the back. One can get concussion also without any contact to the head.

To get an estimate of the relation between impacts to the head and the degree of concussion the prototype device was developed. The device prototype was to measure head impact's linear and rotational acceleration, the data gathered from sensors would then be stored for later analysis and research purposes. The aim of the analysis and research is to find the head stress patterns that are resulting in a concussion [1.].

3.4 Physics Behind Concussion

To understand the nature of a concussion, it is crucial to understand the physics behind head impact that leads to concussion. Concussion is induced by a strong external biomechanical force, that causes the sudden acceleration of the brain within the skull. Recent studies showed that rotational accelerations, which were not thought to play a major role in causing concussion in the past, are also often a root cause for a concussion, just like the linear accelerations.

A brain is suspended within a skull, and is surrounded by cerebrospinal fluid, which serves as a layer of protection between the brain and the skull. When the brain is impacted by a strong external force, the cerebrospinal fluid is unable to prevent it from colliding with the skull. A concussion is an injury that comes as a result of the brain misplacement and direct contact with the skull, resulting bruising, tearing, and swelling of the neural tissue [3.].

There are three types of head injuries: direct injury, acceleration-deceleration injury, blast injury. Figure 1 represents three types of head impacts and every one of them has linear and/or rotational acceleration forces involved, but in different proportions. First is a direct impact, it usually happens when a player's head hits an object like another player's head, ball, or ground. Direct impacts involve linear accelerations and very seldom rotational accelerations. Second is acceleration-deceleration injury, it usually occurs when a player's head is affected indirectly but it still experiences large forces, for example, if a player gets hit to a stomach and a head moves back and forth abruptly after the incident. Acceleration-deceleration injury usually involves both linear and rotational accelerations at the same time. Third is blast injury, it frequently occurs when the player's head is injured indirectly in the same way as in acceleration-deceleration injury, but the acceleration changes more rapidly than in acceleration-deceleration injury. For example, when a player's chest is hit and the head experiences an indirect impact, in whiplash movement. Blast injuries include rotational accelerations and very seldom linear accelerations [7.].

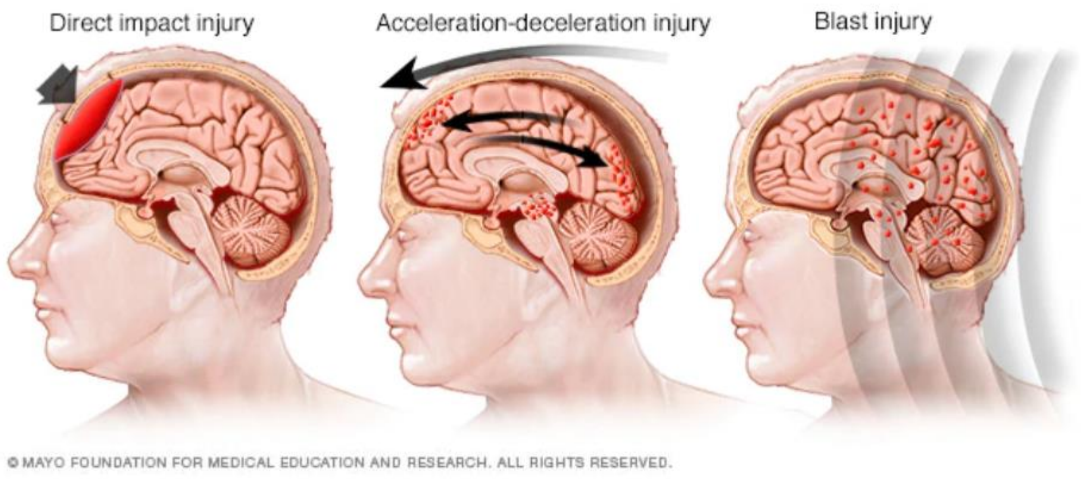

© MAYO FOUNDATION FOR MEDICAL EDUCATION AND RESEARCH. ALL RIGHTS RESERVED.

Figure 1. Three types of head impact [3].

Newtonian formulas can be applied to describe linear and rotational vector forces on the head and brain which cause a concussion. The following formulas can help in calculating the forces of stress on neural tissue under various play and practice conditions. The severity of head injury can be then determined using the results of the formulas. Further calculations can be derived to predict the potential for neurocognitive impairment.

Acceleration - this is a key quantity when describing the forces applied in a mild concussion. The formula for calculating acceleration is as follows:

$$a = \frac{(v^2 - v_0^2)}{2*s*g} \qquad (1)$$

In the formula (1) [8]:

- a is an average acceleration or deceleration over a finite time in meters per second squared.
- v_0 is an initial speed is meters per second.
- v is a final speed meters per second squared.
- s is the distance traveled over a finite time in meters.
- g or g force is gravity acceleration which is applied over an object. One g force is equivalent to 9.812 m/s^2. (g force)

This formula could be applied to video recordings of plays of any contact sport, including ice hockey, football, wrestling, rugby, etc. Using these video recordings, velocities and halting displacements can be calculated. For instance, if a player is running at 4 m/s and his or her head is brought to a stop in 0.2 m, the following acceleration then is calculated:

$$a = \frac{(-4)^2}{2*0.2*9.812} = 4.08\ m/s^2 \qquad (2)$$

In this case, the formula indicates the player's velocity change over time as 4.08g, or more than 4 times the normal acceleration due to gravity, which is 1g. The force on any part of the player's mass (m in kilograms), which experiences an acceleration of magnitude (a) is given by the Newton Second Law of Motion:

$$F = m * a \qquad (3)$$

In the formula 3 [8]:

- F is force measured in Newtons.
- m is mass measured in kilograms.

Let’s suggest that a player is falling to the ground with no other forces affecting him or her aside from gravity force, the Newton Law gives the following:

$$F = m * g \tag{4}$$

For example, if the player experiences an acceleration of 4.08g, the force on any element of mass, for example the brain, is F = (m)*(4.08g). Therefore, the body element experiences 4 times the force of gravity. If the earlier formula of the acceleration is incorporated into the Newton Law, the Law then reads as follows:

$$F = \frac{mv^2}{2*s} \tag{5}$$

The equation in formula (5) suggests that if two collisions have the same initial speed, then the smaller the resulting distance, the bigger the force on the brain. Hence, if a player collides into a fixed object like a fence or ground, the stopping distance will be smaller, which will create a larger force. Larger force means that a potential injury will be more severe.

Apart from linear forces, there are torque vectors that are caused by angled impacts. Previously discussed example cases assume that both players are expecting the collision and are prepared. If the players are unaware of an impact, players may fail to prepare their bodies for the impact e.g. properly tensing the muscles of the back and neck. In such cases, players may experience a jolting force which creates a torque. Torque will cause the head to rotate. Torque formula:

$$\tau = I * \alpha = m * r * \alpha \tag{6}$$

In the formula 6 [9]:

- τ is torque in newton-meters or joule per radian.
- I stands for a moment of inertia measured in kilogram meter squared.
- m stands for mass in kilograms.
- α stands for rotational acceleration in radians per second squared.

Angular acceleration formula:

$$\alpha = \frac{\omega - \omega_0}{t} \qquad (7)$$

In the formula 7:

- α stands for rotational acceleration in radians per second squared.
- ω stands for rotational velocity in radians per second.
- t stands for time in seconds.

Rotational forces can cause rapid velocity changes over short distances, time intervals, or both. When changes in velocity (acceleration) are large, occur in a very short interval, and occur over short distances, in many cases the resulting injuries are more severe than those from linear impacts [8.].

3.5 Head Impact Telemetry System

Head Impact Telemetry System (HITS) is a system including hardware and software intended to detect and measure head impacts in contact sports with a method of accelerometry. HITS can be helmeted and non-helmeted. Helmeted systems, as a name states, are mounted on a helmet. Non-helmeted devices usually installed behind the ear or are embedded into a mouthguard [10.]. Because helmeted HITS proved to be more accurate than non-helmeted, the device prototype was developed to be a helmeted-HITS [11].

Below Figure 2 represents helmeted and non-helmeted wearable devices possible locations. The first picture shows that the helmeted device that is placed on top of the helmet, the second picture represents how a non-helmeted device that is placed in the mouthguard and third picture represents another location option for a non-helmeted device - behind the ear.

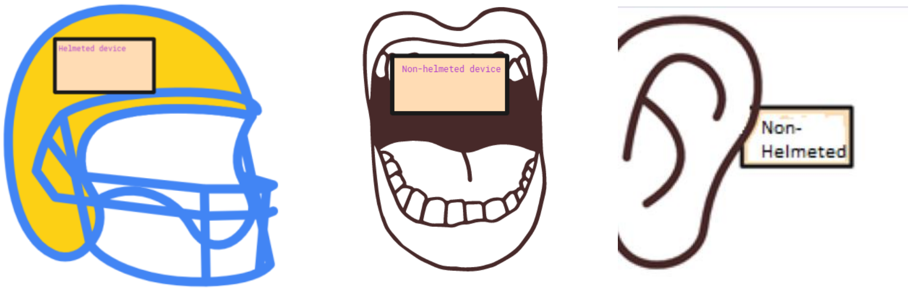

Figure 2. Wearable helmeted and non-helmeted devices possible locations.

3.6 Empirical Studies

Stanford University research aimed to calculate metrics that would be specific to American football. For that reason, the research was focused on assessing a head impact exposure in American players during the plays. The researchers developed a non-helmeted wearable device that helped in collecting the number of head impacts and the kinematics of head impacts from American football players. The device was installed in a mouthguard. The collected data helped in quantifying and developing the metrics.

In previous studies HITS (head impact telemetry system) was used to collect data on hundreds of thousands of impacts over the past decade, and the impact data obtained from these studies was used to determine injury thresholds and develop helmet test protocols. However, later studies have shown that HITS and other wearable sensor systems were not accurate enough in neither counting the head impacts nor measuring the severity of head impacts. The reason for that lied in numerous false-positive impacts recorded by wearable sensors and disregard for repetitive small value impacts, which are known to cause a concussion. In addition, rotational acceleration was known to cause a concussion, and the previous researches were missing valuable rotational acceleration and velocity values, because the collected data had only linear acceleration values.

A video assessment method and gyroscope sensor were used to improve the accuracy of the data and verify the data among the sensors. Also, a smaller threshold was set than in the previous studies. The threshold to be 10 g. Impacts a bit over 10 g do not cause a concussion, but, as it was mentioned earlier, when they are maintained for a long period of time they can result in a concussion.

First the wearable sensors and video assessment results were analyzed separately to eliminate bias and then they were analyzed together. It was found that video assessment significantly improved head impact detection. Also, American football players were equipped with instrumented mouthguards and were recorded on video over the fall season in both practices and games.

The wearable instrumented mouthguard had a PCB which included gyroscope board featuring ± 500, ± 1000, ± 2000, ± 4000 rad/s, and accelerometer board featuring ± 100 g, ± 200 g, ± 400 g.

The wearable instrumented mouthguard recorded impacts to the head when a linear acceleration reached 10 g threshold, and the impacts were registered 10 ms before and 90 ms after the trigger. Because players often removed the instrumented mouthguard while on the sideline, the mouthguards were fitted with an IR proximity sensor that detected the presence of teeth in a mouthguard tray. This way only data from the play was recorded.

In order to collect the data from the play, the wearable sensors and video recording were synchronized. Video assessment protocol used a multi-angle video for a better view of players during the game. Videos were taken from multiple angles to capture impacts more precisely and to avoid any obstacles which could obstruct them from the camera. On the field, there were at least two cameras: one was recording an end-zone and another one capturing a sideline view.

As a result, the independent study of video and mouthguard assessments concluded that 93.8% of video assessed impacts and 85.8% of mouthguard assessed impacts occur to the front, front oblique, and sides of the head. The research found that there were more head impacts per player per play during games than during practices. It was discovered that the mouthguard kinematics device predicted impact location correctly only in 37.3% of the time. On the other hand, the traditional linear acceleration process's impact location predictions were correct 28.1% of the time. The accuracy of prediction was improved with the integration of gyroscope and video assessment [12.].

This thesis work planned to develop an almost identical device- device prototype with 10 g threshold, linear acceleration, rotational acceleration, and velocity measurement devices. The only difference was that the device prototype was of a helmeted HITS type. It was an improvement to the design mentioned in this study, because as it was mentioned earlier helmeted devices proved to be more accurate than non-helmeted. The video assessment tool development was not implemented during the thesis work, but the video assessment tool was planned to be implemented in the future.

4 Requirements

Using the similar methods and approach as in the research conducted by Stanford University, this thesis focused on developing a prototype which would help in collecting data from hockey players, the collected data will then be used to calculate custom metrics to hockey players. The metrics can then be used to better monitor and manage hockey players so that they are less susceptible to potentially dangerous head impact events.

As it was mentioned earlier the idea was to improve the system used in Stanford University research by making the system helmeted. The corresponding plan was developed:

- To develop a device prototype that would allocate and measure the head impact.
- Send the obtained data via wireless communication protocol to the collecting device (e.g. smartphone or raspberry pi).
- Store and process the collected data for further analysis, the data was to be analyzed with the help of medical experts in head injuries.

This chapter describes the first two stages of the plan and planning for the third stage and possible future improvements and requirements descriptions.

In this chapter, potential components and tools were listed, compared, analyzed and selected for the development. The chapter includes a set of requirements for every selected component or tool.

Device prototype requirements:

- The device was to use as little power as possible, since it’s a wearable device was to be used for a long time.
- The device was to be compact and light since it was to be installed on a helmet.
- The device was to be standalone.

Wireless communication requirements:

- Wireless communication’s range had to be as large as the hockey field (around 91.4 to 55.0 meters squared) or larger. [13]

Processor and or chip OS requirements:

- High-performance speed capability.

- On-chip OS or system was to be real-time and event-driven.

Accelerometer requirements:

- The range was to be greater than ± 10 g.

- The range was to be greater than 95th percentile of head impact linear acceleration range in contact sports.

Gyroscope requirements:

- Greater than the 95th percentile of head impact rotational acceleration and/or velocity range areas in contact sports.

Power supply requirements:

- Small size.

- High durability.

Processor sensor communication protocol requirements:

- Communication protocol requirements depended on the selection of sensors. The communication protocol list of the selected sensors was SPI and I2C.

5 Hardware System

The following bill of hardware tools and materials was used for the final prototype: ARM Cortex M4 processor-based chip, BLE5 communication wireless protocol, I2C communication bus protocol, 3-Axes accelerometer and/or 3-Axes gyroscope boards, a mobile phone with BLE support and Android application as an interface for data transmission and reception.

The hardware architecture design can be found below in Figure 3. The hardware architecture and the architecture which involved both hardware and software in black color, while software architecture is in grey color.

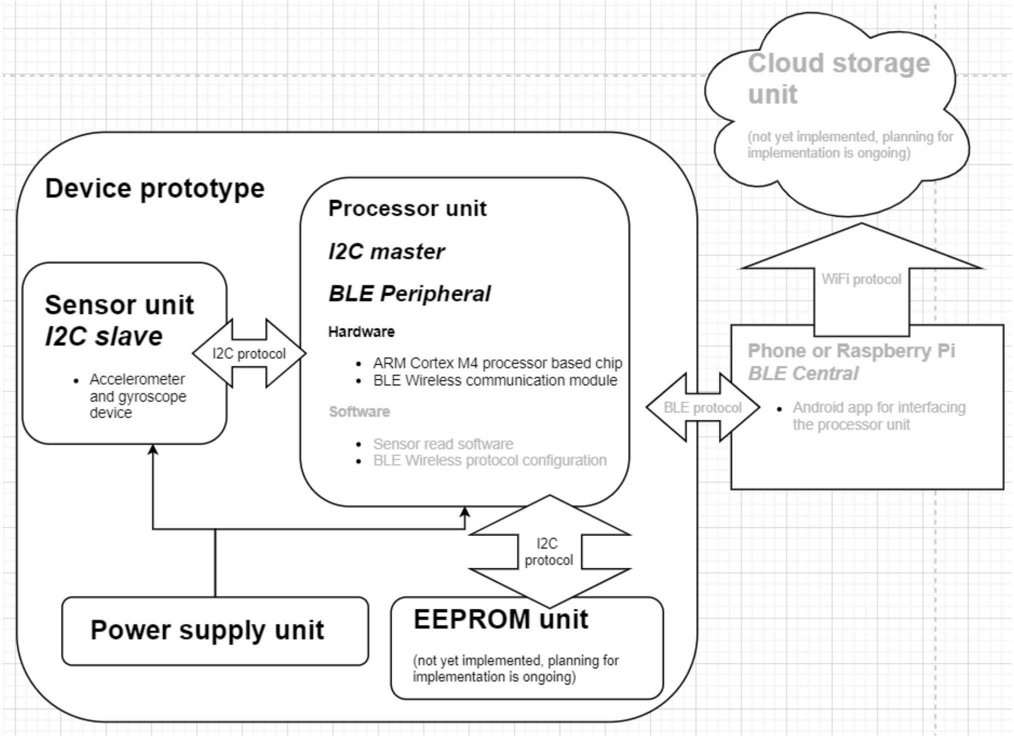
Cloud storage unit
(not yet implemented, planning for implementation is ongoing)
WiFi protocol
Device prototype
Processor unit
I2C master
BLE Peripheral
Hardware
ARM Cortex M4 processor based chip
BLE Wireless communication module
Software
Sensor read software
BLE Wireless protocol configuration
Sensor unit
I2C slave
Accelerometer and gyroscope device
I2C protocol
BLE protocol
Phone or Raspberry Pi
BLE Central
Android app for interfacing the processor unit
I2C protocol
Power supply unit
EEPROM unit
(not yet implemented, planning for implementation is ongoing)

Figure 3. Hardware system architecture design

As was noted in the introduction chapter, this thesis work focuses on the software development process of the device prototype. A more detailed description of the hardware system can be found in the thesis work written by a hardware developer colleague [14].

6 Software System

The software designing was performed in three stages: embedded designing, and embedded development and embedded testing. Embedded designing explains functionality and performance implementation planning before development. Embedded programming includes research and development during the development of a prototype. Embedded testing determines testing processes after the first draft of a program or of a part of a program. Embedded software testing stage ensures smooth and bug-free software.

6.1 Embedded Designing

The Embedded system design was dedicated to delivering software that has efficient performance, high speed, and as bug-free as possible. For building a quality design architecture, it was important to choose the right materials for the device prototype and development tools. The selection of components and devices for the device prototype was based on speed and efficiency. The selection of tools was based on ease to use and the tech support of the vendor. Embedded System Development cycle:

1. Embedded system architecture design.

2. Processor selection.

3. Wireless communication protocol selection.

4. Accelerometer and gyroscope device selection.

5. Processor-sensor communication protocol selection.

6. Development environment selection.

7. Operating System selection.

Further description of the design cycle can be found in the following subchapters.

6.1.1 Embedded System Architecture Design

A block diagram in Figure 4 is a representation of an embedded system architecture design. It includes both software and hardware elements. The embedded system architecture and the architecture represents software part and parts which include both software and hardware parts in black color, while the hardware architecture is in grey color. The unit names are in bold fonts and the I2C and BLE roles are in italic bold fonts.

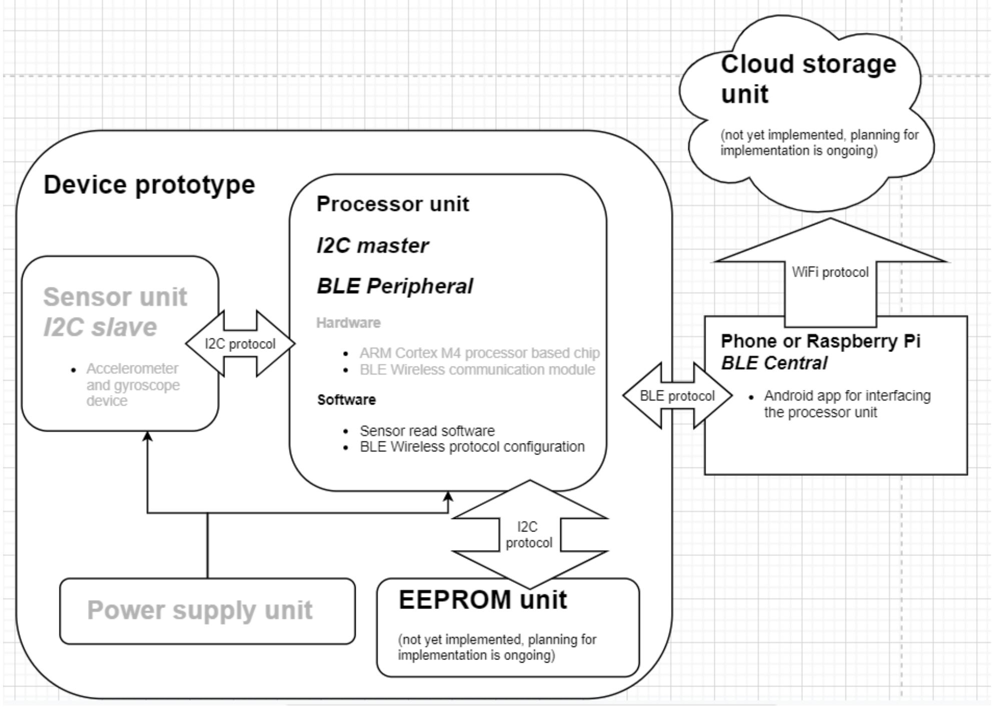
Cloud storage unit
(not yet implemented, planning for implementation is ongoing)
Device prototype
Processor unit
I2C master
BLE Peripheral
Hardware
ARM Cortex M4 processor based chip
BLE Wireless communication module
Software
Sensor read software
BLE Wireless protocol configuration
Sensor unit
I2C slave
Accelerometer and gyroscope device
I2C protocol
WiFi protocol
Phone or Raspberry Pi
BLE Central
Android app for interfacing the processor unit
BLE protocol
I2C protocol
Power supply unit
EEPROM unit
(not yet implemented, planning for implementation is ongoing)

Figure 4. Embedded system architecture design

The processor unit contains embedded system software. The processor software assigned an I2C master role to the processor unit and I2C slave role to the sensor unit. The I2C master role enables the processor to use the I2C communication protocol to obtain the head impact data from the sensor unit which contains accelerometer and gyroscope devices. The processor unit software also manages power, sensor read data rate, processor-sensor communication protocol configurations and data rate, assigns the processor to BLE peripheral role, performs calibration, and sets digitally programmable filters. The processor is responsible for sending data to the central device over the BLE protocol. The power unit supplied the sensor unit and the processor unit with power.

The cloud storage unit and EEPROM data storage unit were not configured during the thesis work and a plan to implement them was in progress. The EEPROM was to serve as an emergency memory storage when the BLE slave to BLE master connection is lost. The cloud storage is used for storing all collected data during hockey games and practices. The data stored in the clouds will be used to help medical professionals to determine the degree of TBI.

6.1.2 Processor Selection

ARM Cortex M4 processor was chosen over other processors, because of its' efficient power consumption and high-performance speed. Processors like AVR have much lower performance speed and use a lot of power.

ARM Cortex M processor series was a better option for the device prototype than ARM cortex A or ARM cortex R processors, because unlike the A and R series processors, it was purposefully designed for low power applications, which is a useful feature for this project since one of the requirements is to use less power.

ARM Cortex M4 processor was designed to have a faster wake up interrupt control interface than other ARM Cortex M processors. An interrupt is a feature that allows a device to better manage power usage. Interrupt is a signal sent to the processor to inform about the event that needs immediate attention. In the case of this thesis work, the processor is in power saving mode when in a normal state, and when the device prototype detects acceleration greater than 10 g the interrupt signal is sent to a processor, then the processor wakes up from sleep mode and handles the data processing [15.].

Also, ARM Cortex M4 is one of the most widely deployed processors, which usually means that there is more literature, more articles and more online discussions and support groups on the processor, hence development and debugging would take much less time and it would be easier to build a quality prototype.

6.1.3 Wireless Communication Protocol Selection

Wireless communication protocol serves as a link between a central device (phone, raspberry pi) and a peripheral device (device prototype).

The information presented below in Table 1 includes candidate wireless protocols for collecting data from the device prototype and their specs for comparison purposes. Candidate protocols were BLE, Wi-Fi, Bluetooth, Zigbee. The required number of maximum active connections was 6, because in a hockey team the number of active players per team is 6. All listed communication protocols met the requirement of maximum active connections. As was mentioned earlier the power consumption was to be a little as possible. In Table 1 there were two candidates that consumed the least of the power: BLE and Zigbee. Though Zigbee would have been a great choice, it had compatibility issues. Zigbee is currently not compatible with any of the existing operating systems. BLE has wide operation range [18]. BLE is supported by most of the widely used operation systems. It was inferred that the BLE communication protocol was the best wireless protocol for the device prototype.

Table 1. Wireless communication protocols specifications table.

Wireless protocols →	**BLE [16]**	**Wi-Fi [17]**	**Bluetooth [17]**	**Zigbee [17]**
Specs ↓				
Maximum range	400-1000 m	92 m	100 m	291 m
Power consumption	10 mW	1 W	1 W	100 mW
Throughput speed	2 Mbps	6 Mbps	128-305 kbps	128 kbps
Operating system	Android, iOS, Windows, OS X	Android, iOS, Windows, OS X	Android, iOS, Windows, OS X	not compatible
Topology	mesh and star	star	mesh	mesh
Maximum number of active connections	10	250	10	15

6.1.4 Accelerometer and Gyroscope Device Selection

The selection of accelerometer was based on accelerometer threshold settings of 10 g set in the study held by Stanford University and 95th percentile and head impact linear acceleration threshold value for hockey plays which was 46 g [10].

Since the devices measuring angular acceleration were not manufactured, it was decided to use a rotational velocity sensor instead. In many previous researches head impact in hockey plays were represented with angular acceleration units, even though the sensors used in the research were gyroscope sensors that measured angular velocity. Therefore, the selection of gyroscope was based on gyroscope median velocity range in football players of 8.5 rad/s - 10.2 rad/s and based on hypothetical rotational velocity threshold for losing consciousness 33 rad/s (4500 rad/s^2 acceleration threshold respectively.). The selected gyroscope range was to be larger than ± 33 rad/s [12.] [19.].

6.1.5 Processor-Sensor Communication Protocol Selection

Below Table 2 represents I2C and SPI communications specifications. I2C communication protocol was used during the device prototype development, because unlike SPI protocol, which is a 4 and more wires protocol, it is a two-wire communication protocol which reduces the complexity of the PCB design. I2C is cheaper and less susceptible to noise than SPI. I2C has a clock stretching feature and SPI doesn’t have it. Clock stretching is helpful when one of the slave devices cannot keep up with the clock, which makes sure that all data is read accurately, and no read data is lost. Acknowledge feature in I2C ensures that the data is successfully received and sent, which is a big advantage when it is crucial to save all the read data with minimal losses.

Table 2. I2C and SPI comparison table.

Communication protocols →	**I2C**	**SPI**
Specs ↓		
Number of master and slave devices	multi-master, multi-slave	one master, multi-slave
Communication protocol type	Half-duplex	Full-duplex
Number of wires	2	3+
Price	Cheap	Costly
Power consumption	more power consumption	less power consumption
Communication speed	Slower	Faster
Noise susceptibility	less susceptible	more susceptible
Clock operation	Clock stretching	no clock stretching
Data insurance	yes, using acknowledge feature	no

However, later during the development process, it became apparent that an SPI communication protocol would have been more suitable, because SPI protocol uses less power than I2C which is important when it comes to wearable sensors. Also, SPI is full duplex which makes it much faster than I2C protocol [20.].

6.1.6 Programming Environment

Arduino IDE was a programming environment where Arduino modules and modules that support Arduino are programmed. The chip that was used in the device prototype was programmed using Arduino IDE. The programming environment uses Arduino programming language which is an implementation of Processing language. The Processing language includes many functions from the C and C++ languages. Arduino programming language is one of the easiest to learn and has a massive amount of support forums online, which speeded up the development process.

More of the Arduino IDE advantages were that it was open source for both hardware and software, which means that it does not require purchasing a license, which is cost – effective. In addition, open source means that it allows a developer to create additional features for his or her project, which would otherwise be impossible with proprietary code. The platform operates on any operating system. The Arduino supporting modules allow a software developer to program a chip using solely USB cable and have a programmer integrated in them, whereas many other modules require an external programmer. Such design is not cost-effective because the programmer is used only during the production phase and is not usually used in the field. When production number increases the integrated programmer in the module adds unnecessary costs. For that reason, the Arduino IDE and an Arduino supporting module were used solely during the prototyping phase, for the future development and improvement another open-source IDE and module were used [21.].

6.1.7 Operation Systems Selection

There was no operation system (OS) selected to be on-chip, because Arduino supporting modules can run a program real-time without OS. Device prototype’s processor was a microcontroller and microcontrollers do not have enough computing power to run on an OS, though it is not impossible, it is not advisable and on-chip OS will slow down the processor’s speed.

The Windows OS was selected for the Arduino IDE, because the Arduino IDE creators support the software for Windows OS. Arduino IDE is more up to date on Windows OS than for Linux OS or iOS and have a bigger support forum groups online for the IDE. Also, most microcontroller systems are limited to Windows OS [22.].

6.2 Embedded system development

Embedded system development's first stage consisted of breakout boards' datasheets analysis. The data provided by datasheets were used in developing breakout boards' libraries. Datasheets instructed on how to implement breakout boards' setup by accessing registers. Below, in the Figure 5 the library configuration setup included the following elements: accessing registers and data handling. Accessing registers stage involved powering up the sensors that were needed for the device prototype, sensors' sample rate setup, sensors' data filtering. Data handling stage involved the conversion of raw sensors' values to metric units and calibration. Arduino IDE has its own I2C library, which was used during the prototype development. BLE protocol supporting libraries were used, which were created by Adafruit company for ARM Cortex M4 based BLE modules.

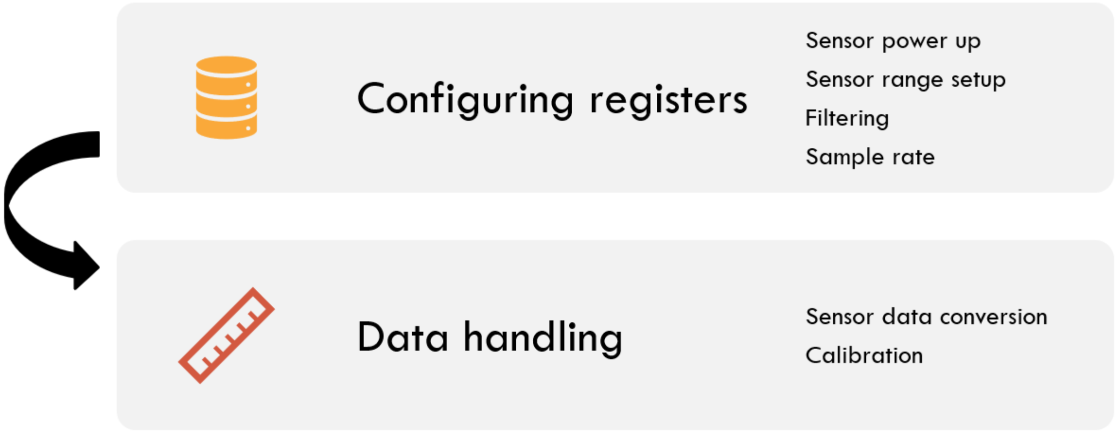

Configuring registers

Sensor power up
Sensor range setup
Filtering
Sample rate

Data handling

Sensor data conversion
Calibration

Figure 5. Library configuration setup elements.

The second stage consisted of building a main program. The main program included breakout boards'/sensor libraries, BLE libraries, I2C libraries, and execution of the main function. Main function contained a loop that fetched the metric sensors data at a certain rate. The below-presented system in Figure 6 describes the main code structure architecture. The system demonstrates setup which included BLE setup I2C configuration steps, followed by BLE pairing cycle, followed by a loop that includes sensor data conversion, sensor data sending over BLE to a mobile phone.

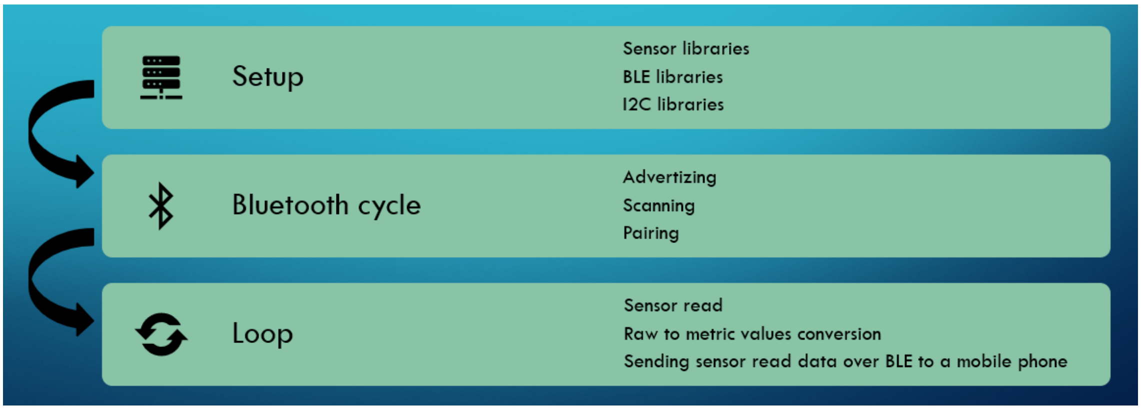

Figure 6. Embedded system main program architecture

There were four candidate breakout boards which were analyzed and compared to be used in the device prototype. Due to the non-disclosure agreement, the thesis cannot reveal the component names, for that reason the devices were labeled with pseudonyms.

1. First device’s features: (let’s call it gadget A)

Gadget A is a breakout board that included both three-axes accelerometer and three-axes gyroscope sensors, digital I2C/SPI serial interface standard output. Gyroscope sensor has digitally programable ranges of ± 250, ± 500, ± 1000, or ± 2000 degrees per second (deg/s) or ± 4.36, ± 8.73, ± 17.45, ± 34.90 rad/s (radians per second). The sample rate is programmable from 8 kHz, down to 3.9 Hz. The three-axes accelerometer featured full-scale ranges of ± 2 g, ± 4 g, ± 8 g, or ± 16 g.

2. Second device’s features: (let’s call it gyroscope board)

Gyroscope board is a breakout board that includes three-axes gyroscope. Gyroscope has ranges of ± 500, ± 1000, ± 2000 or ± 4000 deg/s or ± 8.73, ± 17.45, ± 34.90, ± 69.81 rad/s. As previously stated, the threshold for losing consciousness is ± 33 rad/s, but a gyroscope with a larger range was selected because the rotational forces were recently introduced to measure head impacts in contact sports and they were not well studied yet and therefore it did not have enough data to rely on. Because not enough research was done on rotational forces in head impacts, the gyroscope board was selected for the device prototype. The sample rate of the gyroscope board was programmable from 3.9

Hz up to 8 kHz. Gyroscope board also included a digitally programmable low-pass filter [25.].

3. Third device featured accelerometer: (let’s call it accelerometer board)

Accelerometer board is a low power breakout board. It contains three-axes accelerometer sensor. Accelerometer sensor has a digitally selectable ranges of ± 100 g, ± 200 g, ± 400 g. Output data sample rates are from 0.5 Hz to 1 kHz. As previously stated, the required range for accelerometer sensor was based on the 95th percentile of linear accelerations which was 46 g. Accelerometer board was selected to be a part of a final device prototype.

The gadget A was used in a development process because its setup configurations are like gyroscope and accelerometer boards’. Gadget A was a widely used breakout board device with numerous support forum discussions online, which meant the development process time would be shorter and more efficient. Gadget A was purposefully designed for motion tracking, which meant it would have been perfect for the prototype of a head allocation device if not its accelerometer and gyroscope range limitations. Because of accelerometer board’s fitting accelerometer ranges of ± 100 g, ± 200 g, ± 400 g, it was a better device for the device prototype than gadget A’s accelerometer ranges, which are ± 2 g, ± 4 g, ± 8 g, and ± 16 g. The accelerometer board was used instead for the device prototype, because it had more suitable accelerometer range selection for the device prototype. Libraries and a main code for gadget A were tested and served as a base for the Gyroscope board and Accelerometer board devices.

Gadget B was introduced, and it served as a substitute for the gyroscope board since it was discovered that the manufacturing of the gyroscope board was stopped. Gadget B was a great replacement for the gyroscope board since it had similar gyroscope specifications. In addition, there was an accelerometer sensor with a maximum range of ± 30 g. Even though in the requirements the lowest acceleration threshold was 46 g (the 95th percentile of the impacts) and the gadget B’s maximum range was ± 30 g, the range could be changed from ± 30 g to only + 60 g [10]. Such a solution was considered because it was found that around 93.8 % of impacts occur to the front side of the head [12].

Gadget B had slight differences in memory architecture than gadget A, gyroscope board, or accelerometer board. They had one memory module and gadget B had several memory banks. For that reason, there were several extra lines in the code for switching banks, which slightly affected the computational performance speed of the device prototype and the communication speed.

6.2.1 Libraries development for breakout boards

The libraries for all breakout boards used similar development principle. The development of the libraries began with setting up the transmission over I2C Communication. I2C communication was between processor (master) and breakout board (slave). The full process of I2C communication can be found below in Figure 7. Every small arrow is an 8-bit sequence. Red small arrows stand for data transmission from master to slave and blue small arrows stand for data transmission from slave to master. I2C communication starts with start condition marked with first big arrow and stops with stop condition marked with big arrow in the end. Both start and stop conditions are initialized by the master. After start condition follows a sequence addressing a breakout board with read or write command bit. If the command is to write from a register, then the master writes to register address. For example, power management register address is responsible for turning on the gyroscope and/or accelerometer sensors. If the gyroscope and accelerometer need to be turned on, the power management register will receive a write data command from an I2C master, which will enable the gyroscope and accelerometer. If the command is to read, then the corresponding register provides the data for the I2C master to read. For example, if gyroscope sensor value needs to be obtained, then gyroscope sensor value register will receive a read data command from the I2C master. After every sequence there is dialogue box with an “ACK" which stands for acknowledge bit. Acknowledge is a bit message sent by an I2C slave to reassure I2C master that the sequence was received or sent successfully. The opposite of ACK is NACK which stands for not acknowledge, it happens when data was not successfully received or transmitted, then the I2C communication stops and/or repeats the I2C process again [23.].

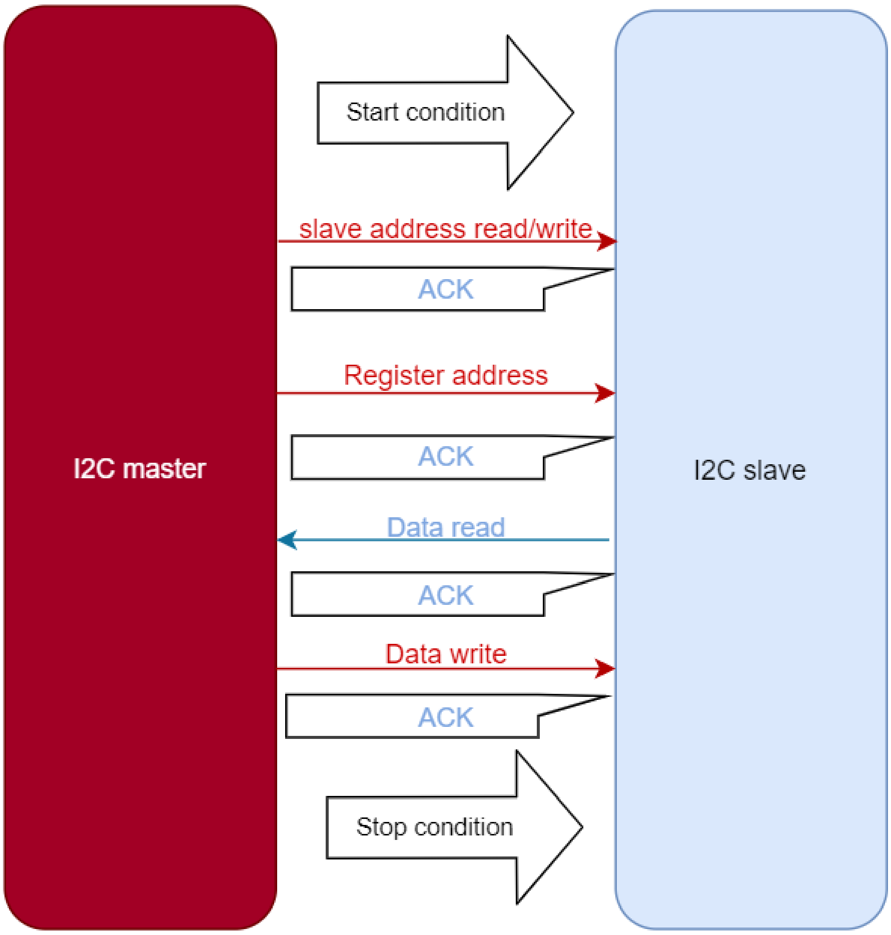

Figure 7. I2C communication process.

During the development of the libraries for breakout boards, I2C master device wrote to the following registers: power management register, I2C management register, accelerometer and gyroscope range configuration registers, digital low pass filter register, accelerometer and gyroscope sample rate registers. Power management register enabled accelerometer and gyroscope sensors. I2C management register actuated I2C bus with the slow 100 kHz mode or fast 400 kHz mode. For the device prototype fast mode was always used.

I2C master device read from the following registers: gyroscope read, accelerometer read. Gyroscope and accelerometer data read registers provide gyroscope and accelerometer sensors' raw data. Gyroscope and accelerometer raw data read from the I2C slave were converted to metric units.

6.2.2 Bluetooth Low Energy Protocol Development

BLE protocol defines four roles: broadcaster, observer, peripheral and central. Broadcaster is a transmitter; it only sends broadcasting data or an advertising packet. Broadcaster's advertising packets are non-collectible which implies that no devices can establish a connection with a broadcaster. One example of a broadcaster is a beacon. The main purpose of broadcasters is to let other devices know about their presence. Observers are receivers and they can receive advertising packets that come from broadcasters and peripheral devices. Observers are non-collectible.

Peripheral devices are devices in a slave role. Peripheral devices can support only one connection. Peripheral devices spread advertising data to let observers and centrals know about their presence and then central devices can choose whether to connect to the peripheral device. A central device is a more complex device than a peripheral device. Central device has a master role and it supports multiple connections. When a device is in a master role it can choose whether to initiate the connection or connections with peripherals, and a peripheral on the other hand, can't choose whether to connect to a master device or not. Single devices may support multiple roles, which means that for instance, an accelerometer board can be a central, a peripheral, an observer and/or a broadcaster at the same time.

Broadcasting data is called advertising. It is the way to let other devices know about your presence and it could be a broadcaster or a peripheral device that advertises. Advertising data are of many types, they can be connectable or non-connectable, scannable or non-scannable. Connectable means that a central accelerometer board can connect to it, and non-connectable means that a central accelerometer board can't connect to it. Advertising can be scannable and non-scannable. Scannable means that a central can request scan response data from a broadcaster without establishing a connection, scan response data is an additional broadcasting data and is always predefined, non-scannable means that a central cannot request for the scan response data from a broadcaster. The device prototype's BLE code had an advertising packet which was connectable and non-scannable.

It is crucial that an observer or a central can recognize a broadcasting device that is usually done by assigning an address to an advertising device. Every BLE device has an address and there are two types of addresses: a random and a public type. The random address is a random number which follows a set of rules set by the Bluetooth special interest group (SIG). There are two types of random addresses- static and private and the difference between the two is the format. A static address is an address that typically will never be changed but it is allowed by the BT SIG to change it upon a power cycle. Private address can either be resolvable or non-resolvable. A resolvable address can change every given interval, for example, every 15 minutes. The resolvable address is changed very frequently in order to avoid the gyroscope board being found by an unknown observer device. Resolvable addresses are generated from an identity resolving key (IRK) and a random number. Only devices that have the IRK distributed by the device using a private resolvable address can resolve that address, allowing them to identify the device. A public address is an address that is in accordance with the 8-bit universal long MAC addresses and must be obtained from IEEE. Public address is unique, and it consists 32 bits. The device prototype's address was configured to be static.

In addition to being able to identify a device, it is also very useful to be able to identify an application or the application that the device has and that is done by advertising universal unique identifiers abbreviated UUIDs. The UUIDs are either 16-bit or 28 bits. The 16 bits UUIDs are used for applications that are defined by the Bluetooth special interest group, for example, heart rate monitor, keyboard, etc. Because there is no defined UUID for neither a tri-axes gyroscope nor for a three-axes accelerometer, a new 28-bit UUID was created for that purpose. During the development process, the sensor data was sent to a central device via BLE print function, and such an approach was not very practical, because, in order for a device with BLE to get certified by SIG, one must obtain UUID for every variable data that is sent over BLE. For data to certify it had to be stored in a variable or variables. The print function was not a variable; hence it was not used for the final device prototype, but it was used during the testing. The BLE data was stored in two one dimensional matrixes each storing 3 variables, one matrix stored accelerometer data, and the other stored gyroscope data. Matrixes were used instead of singular data because it increased the data transmission rate. Also, the BLE has set a maximum data number to 4 variables, in the case of the prototype device, there are 6 variables, to reduce the number of variables we used matrixes. Every variable which was to be sent over BLE received a unique UUID number.

Generic attribute profile or GATT defines a way central accelerometer board communicates with the peripheral device. Attribute protocol or ATT defines how a server's data is constructed and presented to a client. Within the ATT there are 2 roles: client and server.

A client is a device that interacts with the server and reads the server's data. The device prototype was configured to be a server and a mobile phone was a client [24.].

Figure 8 describes the BLE pairing and data retrieving cycle. The device prototype sends advertising data as an advertiser and a mobile phone, as a scanner, reads the advertised packages. Then the mobile phone as a central makes a connection request to the peripheral. Next, when connection is established the device prototype has the role of slave and sends the sensor data to the mobile phone (master).

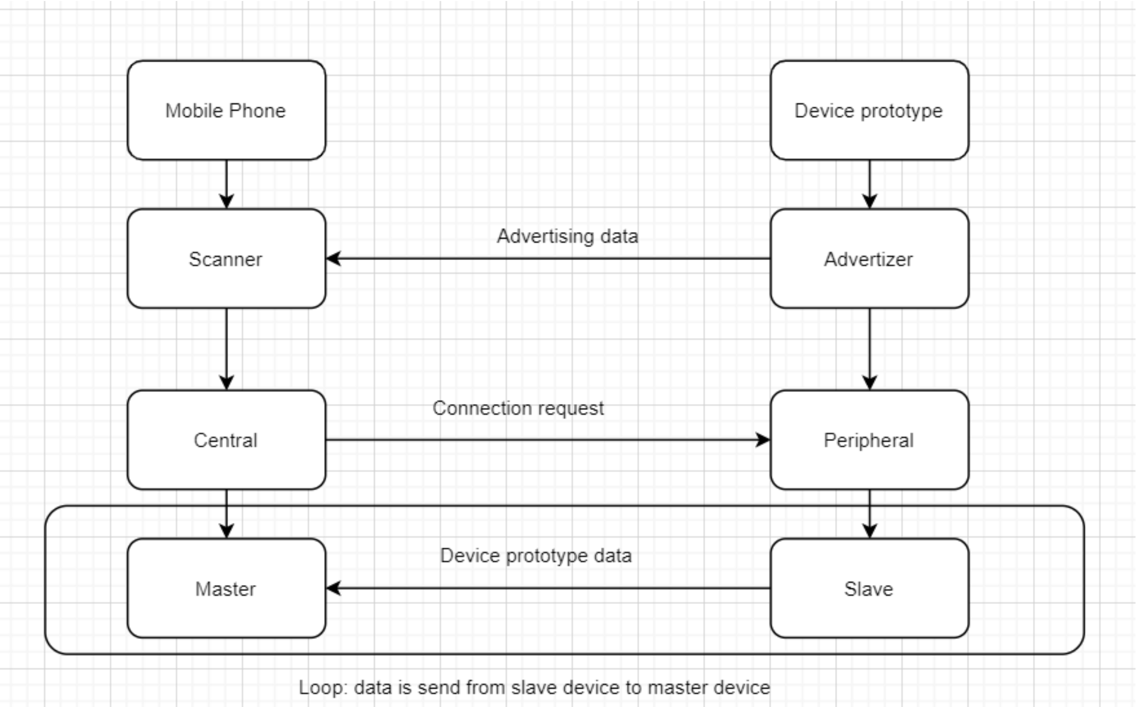

Figure 8. BLE pairing and data retrieving cycle.

6.3 Software testing

Software testing cycle included three parts:

1. Testing of gadget A, gyroscope board, and accelerometer board.

2. Testing of gadget B.

3. Testing of the BLE communication with a mobile application.

Testing setup was done on a flat surface for testing the device prototype’s behavior at rest and in a centrifuge machine to test the device prototype’s behavior when external rotational and linear forces were applied.

6.3.1 Gadget A, accelerometer board, gyroscope board testing

Gadget A settings during testing can be found below in Table 3. In the gadget A’s settings gyroscope was set to the range of ± 2000 deg/s and the accelerometer was set to the range of ± 16 g. Both accelerometer and gyroscope sensors had a sample rate of 1000 Hz. The sensor readings’ results were printed on Arduino IDE’s UART screen with a baud rate of 9600 bits per second (bps).

Table 3. Gadget A settings.

Device's feature name	Settings
Accelerometer's range	± 16 g
Accelerometer's sample rate	1000 Hz
Gyroscope's range	± 2000 deg/s
Gyroscope's sample rate	1000 Hz
Arduino UART baud rate	9600 bps

Accelerometer’s X, Y and Z axes are aligned to the same X, Y, Z directions of the gyroscope within the gadget A. The rotation direction is identified with right-handed screw rule like it is shown in Figure 9. The + x stands for a positive vector and + θ stands for the positive direction of the rotation. If one forms a thumbs-up gesture using the right hand, the thumb will point to the positive direction of a vector and the rest of the fingers will point to a positive direction of the rotation [26].

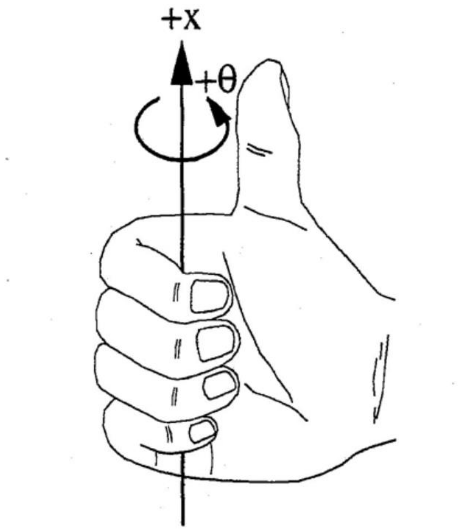

Figure 9. Right-handed screw rule.

Testing setup included placing gadget A on a flat surface with accelerometer’s and gyroscope’s Z-axis pointing downwards while perpendicular X and Y axes were set parallel to the ground like it is shown below in the Figure 10. Earth’s gravitational acceleration direction is marked with a green arrow. Positive parts of the X, Y, Z vector were marked with red lines, while negative parts were marked with blue dashed lines.

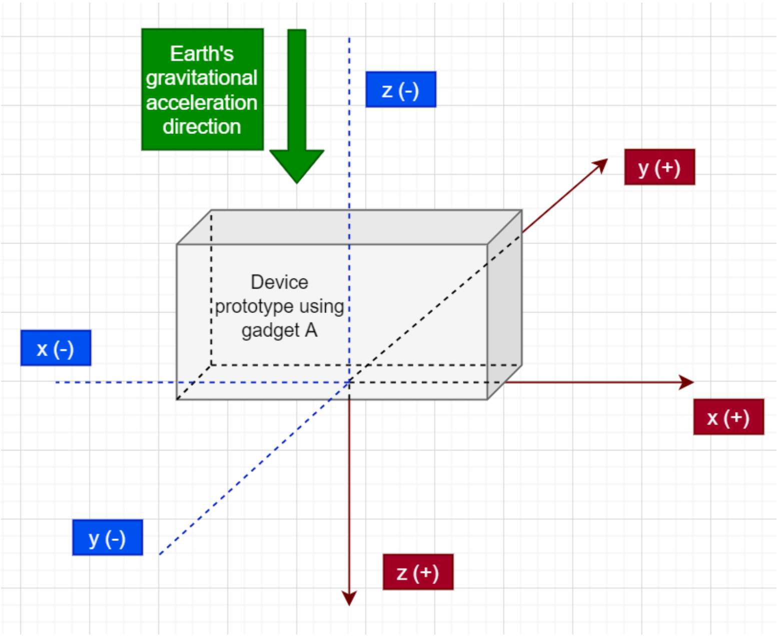
Earth's gravitational acceleration direction
z (-)
y (+)
Device prototype using gadget A
x (-)
x (+)
y (-)
z (+)

Figure 10. Orientation of gadget A during the testing.

The gadget A was tested at rest, which meant that gadget A experienced no rotational velocities and no linear accelerations except for the Earth’s gravitational acceleration of 1 g on Z-axis. Gadget A’s gyroscope experienced no rotational velocities and all axes are at zero. The data which is represented below in Figure 11 were accelerometer and gyroscope.

Marked in blue circle “Gyro (deg)” stands for gyroscope values in degrees per second. An output error is acceptable if it is within a tolerance or nonlinearity ranges. ZRO (zero-rate output) tolerance, which is a tolerance when there are not rotational velocities applied on a breakout board or a sensor, was ± 20 deg/sec.

Marked in red circle is “Accel (g)”, which stands for accelerometer values in g forces. Zero-g is tolerance applied when there are linear accelerations applied on a breakout board or a sensor. The zero-g output tolerance was ± 0.05 g on X and Y axes. The output on X-axis varied from 0.00 g to 0.01 g, which was within the zero-g output tolerance range. The output on Y-axis varied 0.00 g to 0.01 g, which was within the zero-g output tolerance range. Accelerometer nonlinearity was 0.5% of the selected range. The output on Z-axis varied from 1.01 to 1.03 which was within the nonlinearity range, which ranged from 0.92 to 1.08 g.

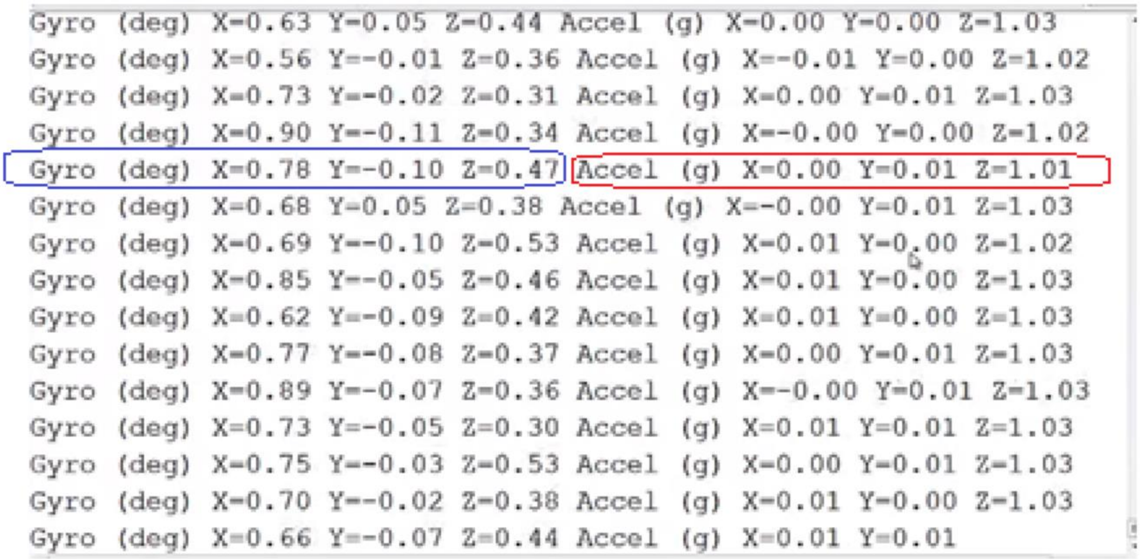

```
Gyro (deg) X=0.63 Y=0.05 Z=0.44 Accel (g) X=0.00 Y=0.00 Z=1.03
Gyro (deg) X=0.56 Y=-0.01 Z=0.36 Accel (g) X=-0.01 Y=0.00 Z=1.02
Gyro (deg) X=0.73 Y=-0.02 Z=0.31 Accel (g) X=0.00 Y=0.01 Z=1.03
Gyro (deg) X=0.90 Y=-0.11 Z=0.34 Accel (g) X=-0.00 Y=0.00 Z=1.02
Gyro (deg) X=0.78 Y=-0.10 Z=0.47 Accel (g) X=0.00 Y=0.01 Z=1.01
Gyro (deg) X=0.68 Y=0.05 Z=0.38 Accel (g) X=-0.00 Y=0.01 Z=1.03
Gyro (deg) X=0.69 Y=-0.10 Z=0.53 Accel (g) X=0.01 Y=0.00 Z=1.02
Gyro (deg) X=0.85 Y=-0.05 Z=0.46 Accel (g) X=0.01 Y=0.00 Z=1.03
Gyro (deg) X=0.62 Y=-0.09 Z=0.42 Accel (g) X=0.01 Y=0.00 Z=1.03
Gyro (deg) X=0.77 Y=-0.08 Z=0.37 Accel (g) X=0.00 Y=0.01 Z=1.03
Gyro (deg) X=0.89 Y=-0.07 Z=0.36 Accel (g) X=-0.00 Y=0.01 Z=1.03
Gyro (deg) X=0.73 Y=-0.05 Z=0.30 Accel (g) X=0.01 Y=0.01 Z=1.03
Gyro (deg) X=0.75 Y=-0.03 Z=0.53 Accel (g) X=0.00 Y=0.01 Z=1.03
Gyro (deg) X=0.70 Y=-0.02 Z=0.38 Accel (g) X=0.01 Y=0.00 Z=1.03
Gyro (deg) X=0.66 Y=-0.07 Z=0.44 Accel (g) X=0.01 Y=0.01
```

Figure 11. Gadget A output values while at rest on a flat surface.

Below Table 4 represents the accelerometer board settings for the testing. In the accelerometer board’s settings accelerometer sensor was set to the range of ± 200 g. The accelerometer sensor had a sample rate of 100 Hz. The sensor readings results were printed on Arduino IDE's UART screen with a baud rate of 9600 bits per second (bps).

Table 4. Accelerometer board settings.

Device's feature name	Settings
Accelerometer's range	± 200 g
Accelerometer's sample rate	100 Hz
Arduino UART baud rate	9600 bps

Testing setup involved placing accelerometer board on a flat surface with accelerometer's Z-axis pointing upwards while perpendicular X and Y axes were set parallel to the ground like it is displayed below in Figure 12. Earth's gravitational acceleration direction is marked with a green arrow. Positive parts of the X, Y, Z vector were marked with red lines, while negative parts were marked with blue dashed lines.

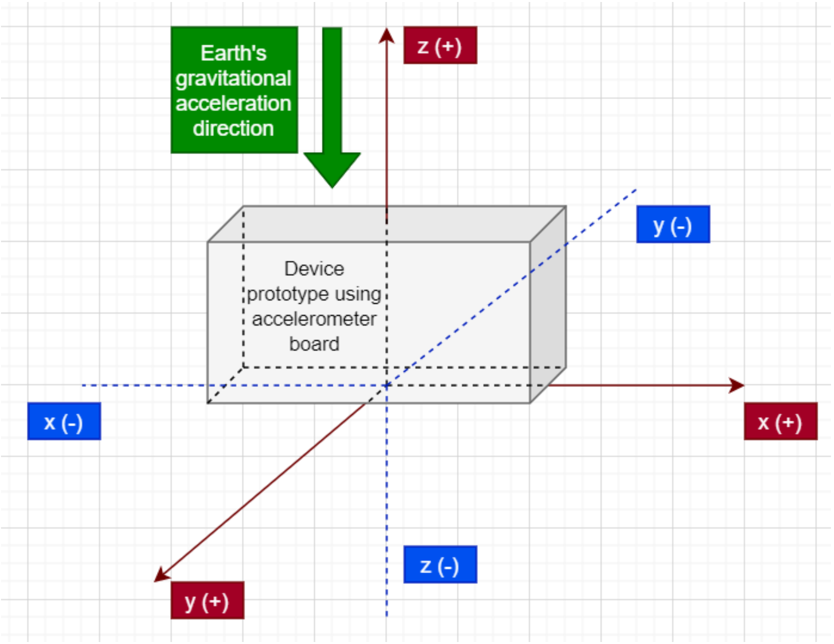
Earth's gravitational acceleration direction
z (+)
y (-)
Device prototype using accelerometer board
x (-)
x (+)
z (-)
y (+)

Figure 12. Accelerometer board's orientation during testing.

The data in the Figure 13 represents raw accelerometer data and accelerometer data in meters per second squared (m/sec^2). Marked with red: first X, Y, Z values stand for the raw data, and latter X, Y, Z stand for accelerometer's converted data in m/sec^2. As it was mentioned earlier accelerometer board was placed upside-down and for that reason data from the linear acceleration value on Z-axis was negative. The zero-g output tolerance was ± 1 g on all axes. The nonlinearity was ± 1 % of the largest range, which equals to

± 1 g. The output on X-axis varied from 0.00 g to 0.01 g, which was within the zero-g output tolerance range. The output on Y-axis varied from 0.00 g to 0.01 g, which was within the zero-g output tolerance range. The output on Z-axis varied from 1.01 to 1.03 which was within the nonlinearity range, which was from 0.5 g to 1.5 g.

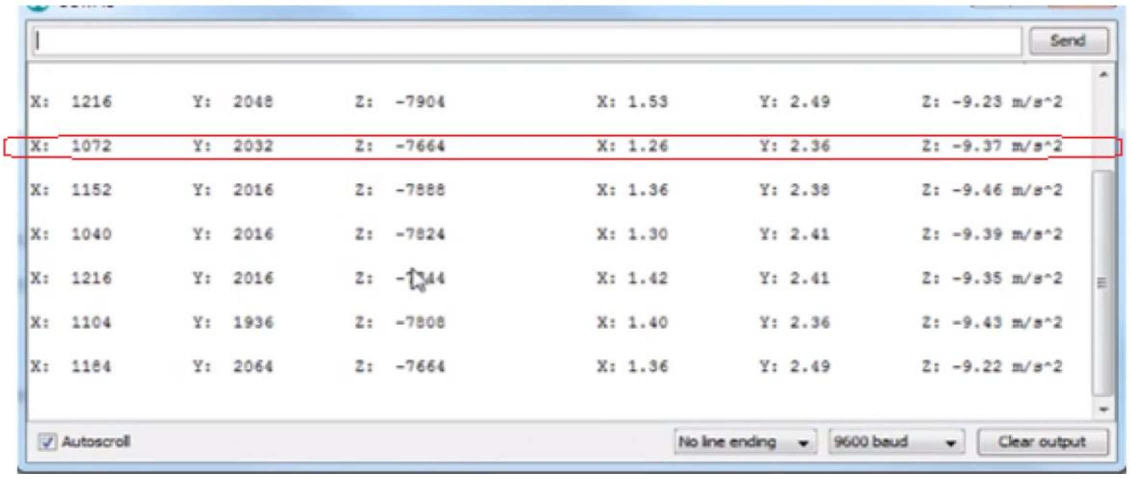

```
X:  1216      Y:  2048      Z:  -7904          X: 1.53      Y: 2.49      Z: -9.23 m/s^2
X:  1072      Y:  2032      Z:  -7664          X: 1.26      Y: 2.36      Z: -9.37 m/s^2
X:  1152      Y:  2016      Z:  -7888          X: 1.36      Y: 2.38      Z: -9.46 m/s^2
X:  1040      Y:  2016      Z:  -7824          X: 1.30      Y: 2.41      Z: -9.39 m/s^2
X:  1216      Y:  2016      Z:  -7[illegible]44          X: 1.42      Y: 2.41      Z: -9.35 m/s^2
X:  1104      Y:  1936      Z:  -7808          X: 1.40      Y: 2.36      Z: -9.43 m/s^2
X:  1184      Y:  2064      Z:  -7664          X: 1.36      Y: 2.49      Z: -9.22 m/s^2
```

Figure 13. Accelerometer board raw output values and converted output values in meters per second squared at rest.

Table 5 below represents gyroscope board settings used during testing. In the gyroscope board's settings gyroscope was set to the range of ± 4000 deg/s. Gyroscope sensors had a sample rate of 8000 Hz. The sensor readings' results were printed on the mobile Adafruit Android application's UART screen with a baud rate of 115200 bits per second (bps).

Table 5. Gyroscope board settings.

Device's feature name	**Settings**
Gyroscope's range	± 4000 deg/s
Gyroscope's sample rate	8000 Hz
BLE UART baud rate	115200 bps

Gyroscope board was tested at rest, on the flat surface area. The gyroscope's X Y Z orientation did not matter, because the gyroscope did not experience any rotational velocities during testing.

Gyroscope's output values at rest were to be 0 deg/s in all axes. In Figure 14 marked with red: first value was an output of X-axis, the second value was output at Y-axis, and the third value was output from Z-axis. All values were in deg/s. The ZRO was ± 15 deg/s for all axes. The biggest variations were 0.37 deg/s and + 0.24 deg/s which were within the ZRO range. the output of the gyroscope successfully matched the expected values. Figure 14 also presents the values in the Android mobile phone application, which indicates that the BLE was implemented correctly and BLE UART communication was established successfully.

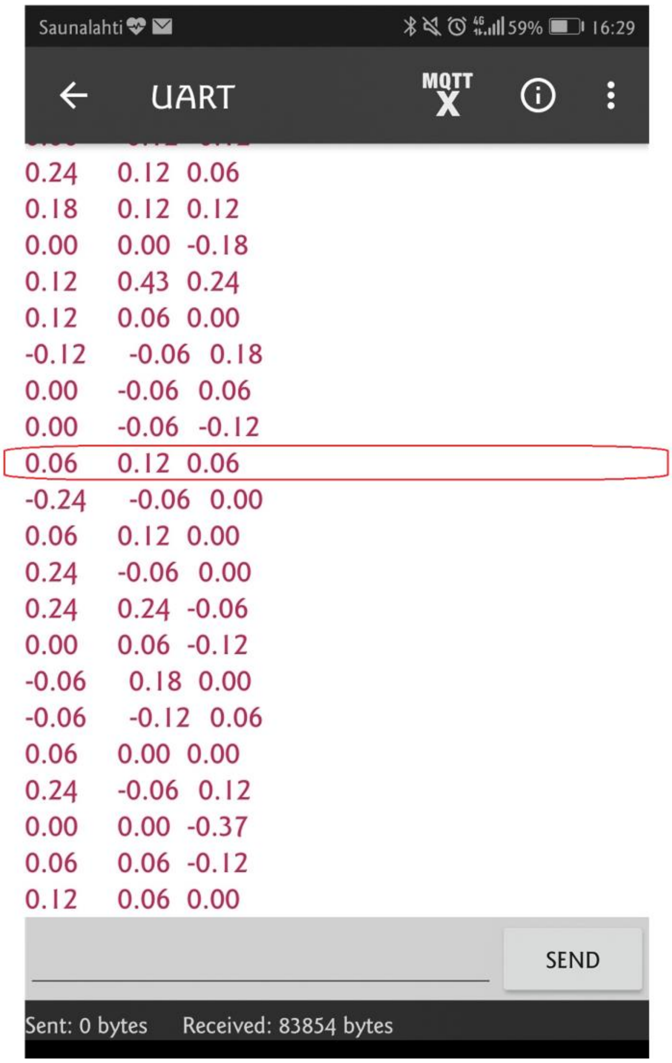

```
0.24    0.12  0.06
0.18    0.12  0.12
0.00    0.00  -0.18
0.12    0.43  0.24
0.12    0.06  0.00
-0.12    -0.06  0.18
0.00    -0.06  0.06
0.00    -0.06  -0.12
0.06    0.12  0.06
-0.24    -0.06  0.00
0.06    0.12  0.00
0.24    -0.06  0.00
0.24    0.24  -0.06
0.00    0.06  -0.12
-0.06    0.18  0.00
-0.06    -0.12  0.06
0.06    0.00  0.00
0.24    -0.06  0.12
0.00    0.00  -0.37
0.06    0.06  -0.12
0.12    0.06  0.00
```

Sent: 0 bytes   Received: 83854 bytes

Figure 14. Gyroscope board’s gyroscope output values at rest in deg/s.

6.3.2 Gadget B and Bluetooth Low Energy testing.

The gadget B configurations can be found below in Table 6. Gadget B was configured to have ± 4000 deg/s range for a gyroscope, and ± 30 g range for an accelerometer, both sampling at a rate of 1000 Hz. The BLE UART baud rate was 115200 bps.

Table 6. Gadget B setup configurations.

Device's feature name	Settings
Gyroscope's range	± 4000 rad/s
Gyroscope's sample rate	1000 Hz
Accelerometer's range	± 30 g
Accelerometer's sample rate	1000 Hz
BLE UART baud rate	115200 bps

Figure 15 below is a representation of the gadget B testing setting with accelerometer's and gyroscope's X, Y, Z orientation. Testing setup included placing gadget B on a flat surface with accelerometer's and gyroscope's Z-axis pointing downwards while perpendicular X and Y axes were set parallel to the ground. Earth's gravitational acceleration direction is marked with a green arrow. Positive parts of the X, Y, Z vector were marked with red lines, while negative parts were marked with blue dashed lines.

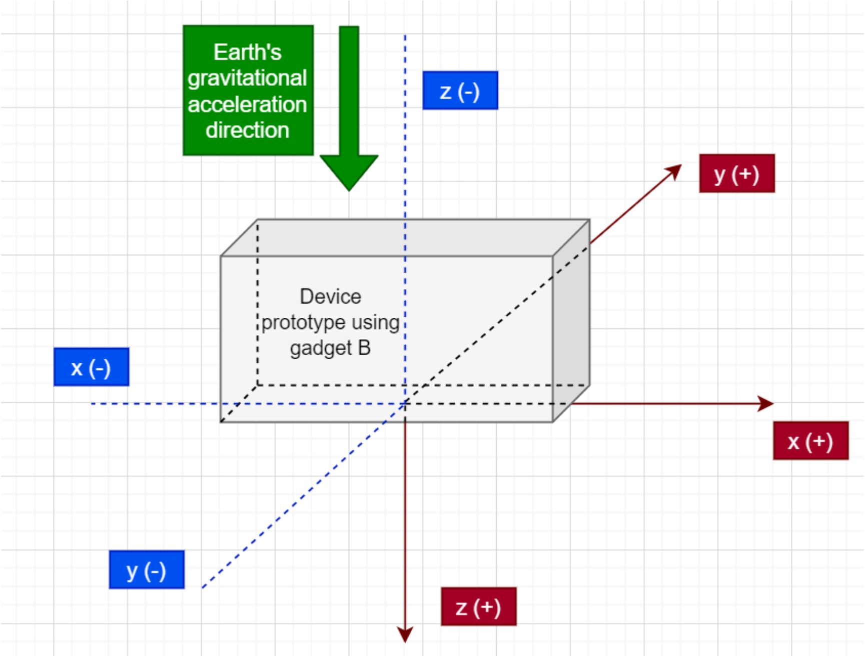
Earth's gravitational acceleration direction
z (-)
y (+)
Device prototype using gadget B
x (-)
x (+)
y (-)
z (+)

Figure 15. Gadget B setup with accelerometer's and gyroscope's X Y Z orientation.

Below in Figure 16 marked with red are the AX, AY and AZ stand for X, Y, and Z axes. The lines marked with red with "ANG" ending stood for gyroscope values in degrees per second. The ZRO range was ± 5 deg/s on every axis. The gyroscope's output varied from - 3.05 to - 2.13 deg/s on X-axis, from 0.85 deg/s to 1.40 deg/s on Y-axis and from - 0.79 deg/s to - 0.18 deg/s which were within the ZRO range requirements. Marked with blue are the lines with "Gforce" endings stand for accelerometer values in g forces. The initial zero-g tolerance range was ± 0.065 g. The output varied from - 0.05 g to - 0.03 g on X-axis, from - 0.04 g to - 0.01 g on Y-axis which were within the tolerance range. The nonlinearity percentage was 0.05 % of the accelerometer's maximum range. By applying the nonlinearity percentage, the expected values on Z-axis are defined to be from 0.85 to 1.15 g. The output on Z-axis varied from 0.96 g to 0.99 g which was within the expected range.

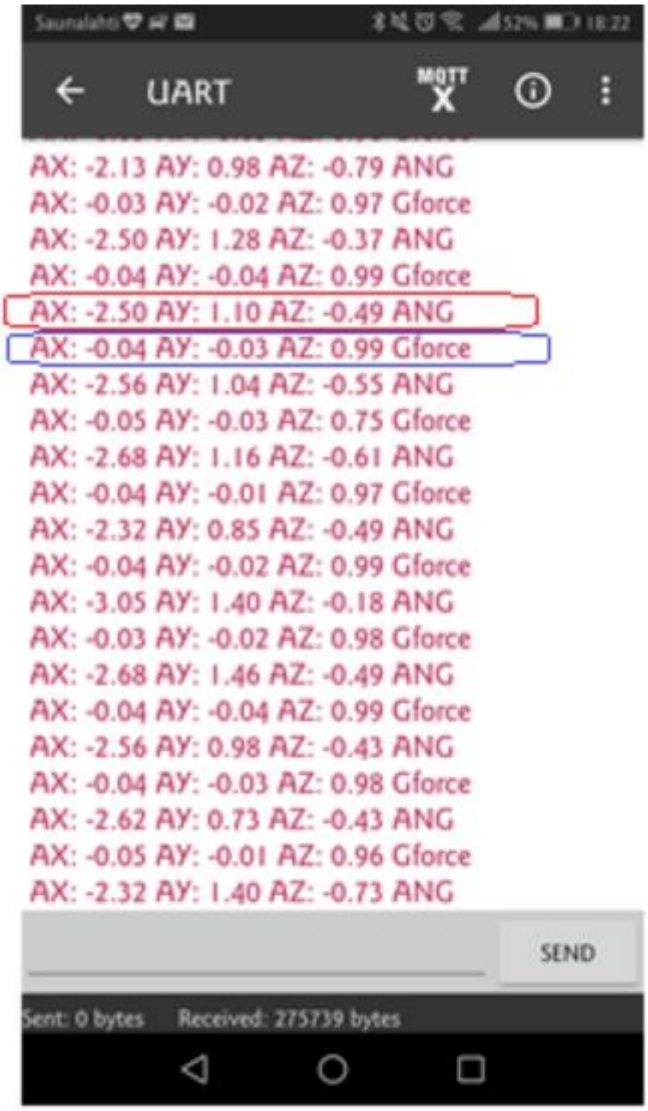

```
AX: -2.13 AY: 0.98 AZ: -0.79 ANG
AX: -0.03 AY: -0.02 AZ: 0.97 Gforce
AX: -2.50 AY: 1.28 AZ: -0.37 ANG
AX: -0.04 AY: -0.04 AZ: 0.99 Gforce
AX: -2.50 AY: 1.10 AZ: -0.49 ANG
AX: -0.04 AY: -0.03 AZ: 0.99 Gforce
AX: -2.56 AY: 1.04 AZ: -0.55 ANG
AX: -0.05 AY: -0.03 AZ: 0.75 Gforce
AX: -2.68 AY: 1.16 AZ: -0.61 ANG
AX: -0.04 AY: -0.01 AZ: 0.97 Gforce
AX: -2.32 AY: 0.85 AZ: -0.49 ANG
AX: -0.04 AY: -0.02 AZ: 0.99 Gforce
AX: -3.05 AY: 1.40 AZ: -0.18 ANG
AX: -0.03 AY: -0.02 AZ: 0.98 Gforce
AX: -2.68 AY: 1.46 AZ: -0.49 ANG
AX: -0.04 AY: -0.04 AZ: 0.99 Gforce
AX: -2.56 AY: 0.98 AZ: -0.43 ANG
AX: -0.04 AY: -0.03 AZ: 0.98 Gforce
AX: -2.62 AY: 0.73 AZ: -0.43 ANG
AX: -0.05 AY: -0.01 AZ: 0.96 Gforce
AX: -2.32 AY: 1.40 AZ: -0.73 ANG
```

Sent: 0 bytes   Received: 275739 bytes

Figure 16. Gadget B's output at rest.

Next test was made by setting the device prototype in a centrifuge machine. The gadget B configurations can be found below in Table 7. Gadget B was set to have ± 2000 deg/s range for a gyroscope, and ± 30 g range for an accelerometer, both sampling at a rate of 8000 Hz. The BLE UART baud rate was 115200 bps.

Table 7. Gadget B setup configurations.

Device's feature name	Settings
Gyroscope's range	± 2000 rad/s
Gyroscope's sample rate	8000 Hz
Accelerometer's range	± 32 g
Accelerometer's sample rate	8000 Hz
BLE UART baud rate	115200 bps

Figure 17 below is a representation of the gadget B testing setup with accelerometer's and gyroscope's X, Y, Z orientation in the centrifuge machine. The blue arrow stands for the direction of rotation in the centrifuge, if viewed from the top then the direction of the rotation is clockwise. Accelerometer's and gyroscope's Z-axis pointing downwards while perpendicular X and Y axes were set parallel to the ground. Earth's gravitational acceleration direction is marked with a green arrow. Positive parts of the X, Y, Z vector were marked with red lines, while negative parts were marked with blue dashed lines.

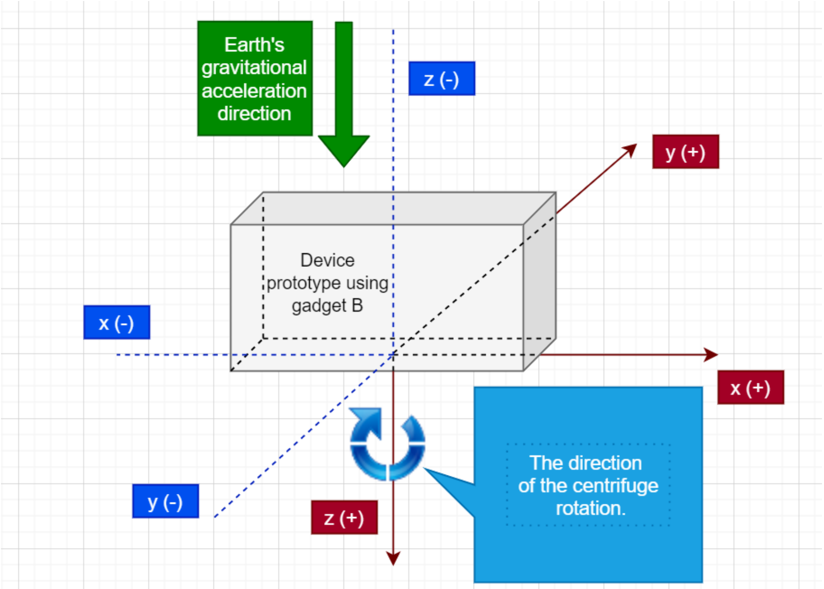
Earth's gravitational acceleration direction
z (-)
y (+)
Device prototype using gadget B
x (-)
x (+)
The direction of the centrifuge rotation.
y (-)
z (+)

Figure 17. Gadget B orientation setup in the centrifuge machine.

Below the Figure 18 shows the centrifuge machine test results in deg/s. The centrifuge testing was intended to assess the maximum ranges of the gyroscope sensor. The centrifuge machine was rotating at the speed of 400 RPM or roughly 2400 deg/s. The lines starting with "angular" followed by "X:", "Y:", "Z:" stand for angular velocity values on X, Y, and Z axes. The output values at the X and Y axes were not at zero because the gadget B was not set completely flat in the centrifuge machine. It can be observed in the line marked in green in Figure 18 that the gyroscope output tended to change polarity after a few seconds, when it reached the range limits. There is a sudden change from + 1998.05 deg/s to - 1998.05 deg/s.

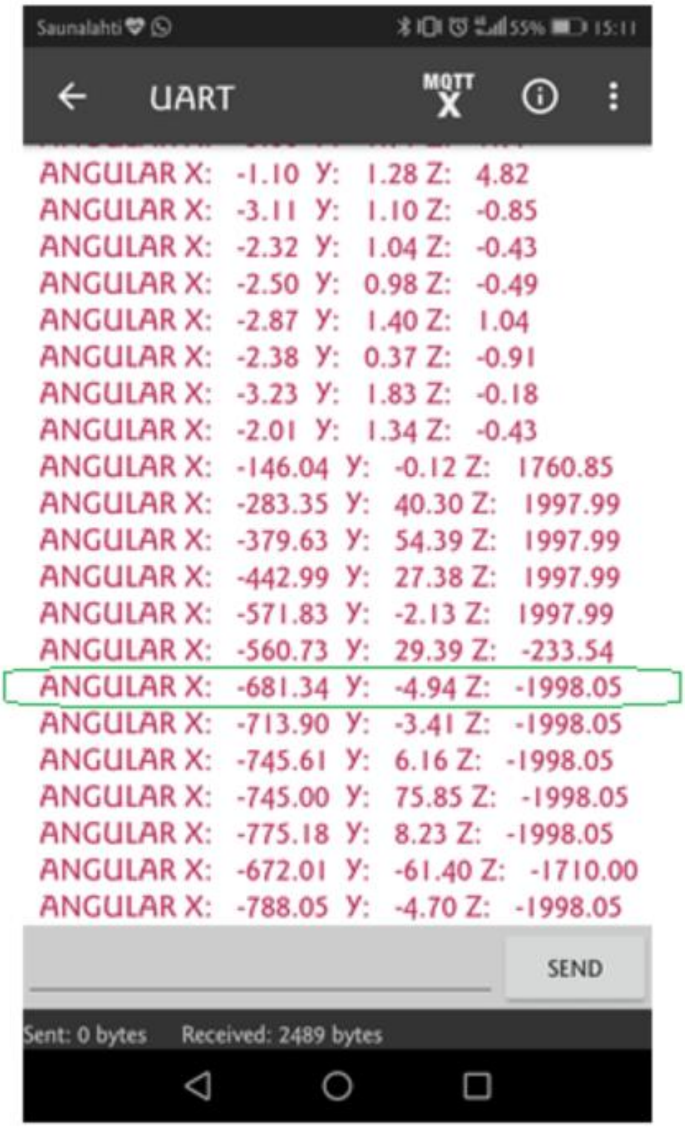

```
ANGULAR X:  -1.10  Y:  1.28 Z:  4.82
ANGULAR X:  -3.11  Y:  1.10 Z:  -0.85
ANGULAR X:  -2.32  Y:  1.04 Z:  -0.43
ANGULAR X:  -2.50  Y:  0.98 Z:  -0.49
ANGULAR X:  -2.87  Y:  1.40 Z:  1.04
ANGULAR X:  -2.38  Y:  0.37 Z:  -0.91
ANGULAR X:  -3.23  Y:  1.83 Z:  -0.18
ANGULAR X:  -2.01  Y:  1.34 Z:  -0.43
ANGULAR X:  -146.04  Y:  -0.12 Z:  1760.85
ANGULAR X:  -283.35  Y:  40.30 Z:  1997.99
ANGULAR X:  -379.63  Y:  54.39 Z:  1997.99
ANGULAR X:  -442.99  Y:  27.38 Z:  1997.99
ANGULAR X:  -571.83  Y:  -2.13 Z:  1997.99
ANGULAR X:  -560.73  Y:  29.39 Z:  -233.54
ANGULAR X:  -681.34  Y:  -4.94 Z:  -1998.05
ANGULAR X:  -713.90  Y:  -3.41 Z:  -1998.05
ANGULAR X:  -745.61  Y:  6.16 Z:  -1998.05
ANGULAR X:  -745.00  Y:  75.85 Z:  -1998.05
ANGULAR X:  -775.18  Y:  8.23 Z:  -1998.05
ANGULAR X:  -672.01  Y:  -61.40 Z:  -1710.00
ANGULAR X:  -788.05  Y:  -4.70 Z:  -1998.05
```

Figure 18. Angular velocity output in deg/s of gadget B in the centrifuge.

A complaint on the matter was written to a manufacturer. The manufacturer responded that the polarity change was the manufacturer’s fault and that they received dozens of complaints on the same issue. As a result, it was found that the reason for the gyroscope sensor’s sudden change in polarity was not due to a bug in the software for the device prototype.

Later software solution was implemented to solve the issue with software polarity change. The results can be found below in Figure 19. The results were obtained with a similar test setup as in previous testing of gadget B. The lines marked in yellow have the “Gforce” ending represent the accelerometer’s data in g, the line marked in blue with “ANG” ending represent gyroscope’s data in deg/s.

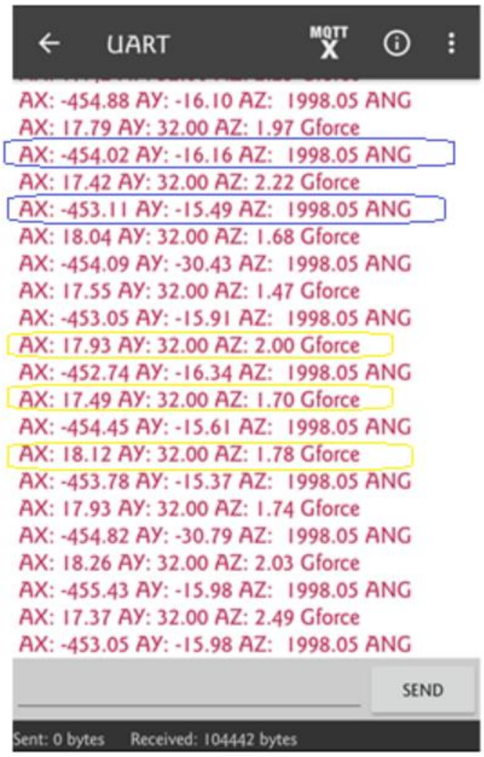

```
AX: -454.88 AY: -16.10 AZ:  1998.05 ANG
AX: 17.79 AY: 32.00 AZ: 1.97 Gforce
AX: -454.02 AY: -16.16 AZ:  1998.05 ANG
AX: 17.42 AY: 32.00 AZ: 2.22 Gforce
AX: -453.11 AY: -15.49 AZ:  1998.05 ANG
AX: 18.04 AY: 32.00 AZ: 1.68 Gforce
AX: -454.09 AY: -30.43 AZ:  1998.05 ANG
AX: 17.55 AY: 32.00 AZ: 1.47 Gforce
AX: -453.05 AY: -15.91 AZ:  1998.05 ANG
AX: 17.93 AY: 32.00 AZ: 2.00 Gforce
AX: -452.74 AY: -16.34 AZ:  1998.05 ANG
AX: 17.49 AY: 32.00 AZ: 1.70 Gforce
AX: -454.45 AY: -15.61 AZ:  1998.05 ANG
AX: 18.12 AY: 32.00 AZ: 1.78 Gforce
AX: -453.78 AY: -15.37 AZ:  1998.05 ANG
AX: 17.93 AY: 32.00 AZ: 1.74 Gforce
AX: -454.82 AY: -30.79 AZ:  1998.05 ANG
AX: 18.26 AY: 32.00 AZ: 2.03 Gforce
AX: -455.43 AY: -15.98 AZ:  1998.05 ANG
AX: 17.37 AY: 32.00 AZ: 2.49 Gforce
AX: -453.05 AY: -15.98 AZ:  1998.05 ANG
```

Sent: 0 bytes Received: 104442 bytes

Figure 19. Software solution results for polarity change problem.

In addition, in the Figure 19 the accelerometer sensor experiences centripetal acceleration. Centripetal acceleration on X-axis is varying from 17.37 g to 18.26 g, on Y-axis stays at 32 g and on Z-axis varies from 1.47 g to 2.49 g. Average centripetal acceleration for X and Z-axis was derived from 1000 readings while applying steady 400 RPM (2400 deg/s) rotational velocity, the Y-axis was not averaged because it experienced acceleration larger than the maximum range. The results were 17.8 g for X-axis and 2 g for Z-axis. As was mentioned earlier the nonlinearity was 0.5% of the maximum range. The deviation can range from 17.65 g to 17.95 g on X-axis and from 1.85 g to 2.15 g on Y-axis. Even though the output results did not fit to the expected ones, it was concluded the sensor experienced minor additional vibrations due to wobbly positioning of the breakout board in the centrifuge machine. Hence it was concluded that the centripetal acceleration on X-axis and Y-axis were stable. The gyroscope does not reach + 2000 deg/s on Z-axis and the accelerometer goes over the maximum range of + 30 g on Y-axis because the range of ± 2000 deg/s and ± 30 g specified in datasheets are theoretical approximations of the maximum ranges.

By knowing the formula for centripetal acceleration, we can determine how far from the center the device prototype was located and how flat or not flat the device prototype was set in the centrifuge machine. It can also be noted that the centripetal acceleration is steady on X and Y axes which means the rotational velocity is steady because centripetal acceleration and rotational velocity are directly proportional. Such results were expected because the centrifuge machine had a steady rotational velocity. Thence, both accelerometer and gyroscope passed the testing successfully.

To improve the gyroscope accuracy a digital low pass filter was added to the device prototype software design. According to studies conducted to determine best frequency for head impact measurement, the device prototype had to be able to measure impacts duration events of 7 ms and bigger. This meant that the best digital low pass filter range had to be bigger than 142.9 Hz. There were two options that were suitable: 151.8 Hz low pass filter and 196.6 Hz low pass filter. It was decided to use the former one. In Table 8 setup configurations can be found [27]. In the gadget B's settings gyroscope was set to the range of ± 2000 deg/s. Gyroscope was sampled at a rate of 1000 Hz. The sensor readings results were printed on Arduino IDE's UART screen with a baud rate of 115200 bps.

Table 8. Setup configurations with digital low pass filter

Device's feature name	**Settings**
Gyroscope's range	± 2000 rad/s
Gyroscope's sample rate	1000 Hz
Arduino UART baud rate	115200 bps
Digital low pass filter frequency 3 dB BW for Gyroscope	151.8 Hz

In Figure 20 setup orientation can be found. Testing setup included placing gadget B on a flat surface with accelerometer's and gyroscope's Z-axis pointing downwards while perpendicular X and Y axes were set parallel to the ground. Earth's gravitational acceleration direction is marked with a green arrow. Positive parts of the X, Y, Z vector were marked with red lines, while negative parts were marked with blue dashed lines.

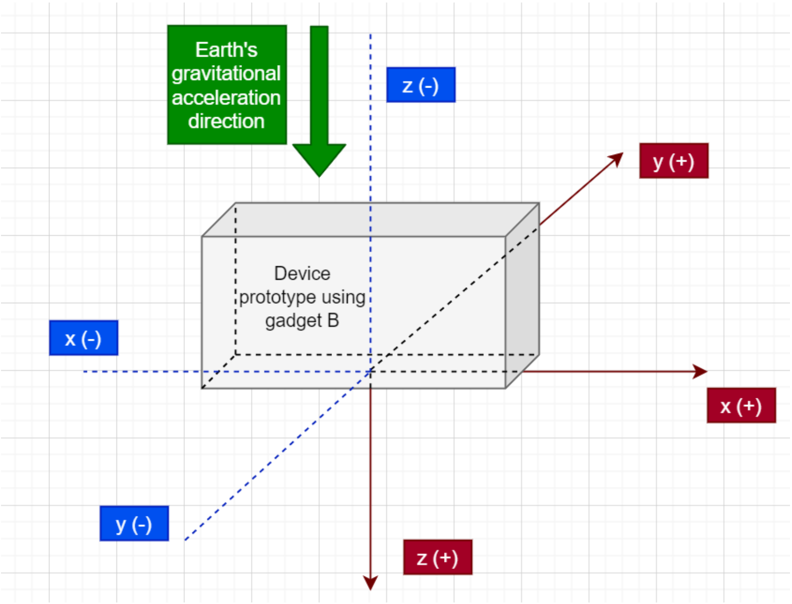
Earth's gravitational acceleration direction
z (-)
y (+)
Device prototype using gadget B
x (-)
x (+)
y (-)
z (+)

Figure 20. Gadget B setup orientation during testing, when digital low pass filter is applied.

The test results showed that the accuracy improved drastically. Below, in Table 9 the gadget B gyroscope with digital low pass filter results are shown. The deviation now is now drastically smaller. The ranging with low pass filter on X-axis was from - 0.3 deg/s to -0.15, on Y-axis was from - 0.1 deg/s to 0 and on Z-axis was from 0.01 deg/s to 0.05 deg/s. The ranging without low pass filter were - 3.05 to - 2.13 deg/s on X-axis, from 0.85 deg/s to 1.40 deg/s on Y-axis and from - 0.79 deg/s to - 0.18 deg/s. The results were printed on Arduino UART screen and logged manually to Table 9.

Table 9. Gadget B results with digital low pass filter at rest printed in Arduino UART.

x	y	z
- 0.3 deg/s	- 0.1 deg/s	0.02 deg/s
- 0.2 deg/s	0 deg/s	0.01 deg/s
- 0.15 deg/s	0 deg/s	0.05 deg/s
- 0.2 deg/s	0 deg/s	0.01 deg/s
- 0.21 deg/s	- 0.1 deg/s	0.01 deg/s

In the last phase BLE GATT functionality for sending and receiving variable values was developed. The setup for gadget B with BLE GATT setup can be found below in Table 10. While most of the setup configurations remained the same as in the previous testing, BLE GATT was sampled at 9600 bps baud rate. In the settings, gyroscope was set to the range of ± 2000 deg/s and the accelerometer was set to the range of ± 16 g. Both accelerometer and gyroscope sensors had a sample rate of 1000 Hz. The sensor readings results were sent to an Android application using BLE GATT with a baud rate of 9600 bits per second (bps).

Table 10. Gadget B with BLE GATT functionality setup.

Device's feature name	**Settings**
Accelerometer's range	± 16 g
Accelerometer's sample rate	1000 Hz
Gyroscope's range	± 2000 deg/s
Gyroscope's sample rate	1000 Hz
BLE GATT baud rate	9600 bps
Digital low pass filter frequency 3 dB BW for Gyroscope	151.8 Hz

The orientation of gadget B can be found below in Figure 21. Testing setup included placing gadget B on a flat surface with accelerometer’s and gyroscope’s Z-axis pointing downwards while perpendicular X and Y axes were set parallel to the ground. Earth’s gravitational acceleration direction is marked with a green arrow. Positive parts of the X, Y, Z vector were marked with red lines, while negative parts were marked with blue dashed lines.

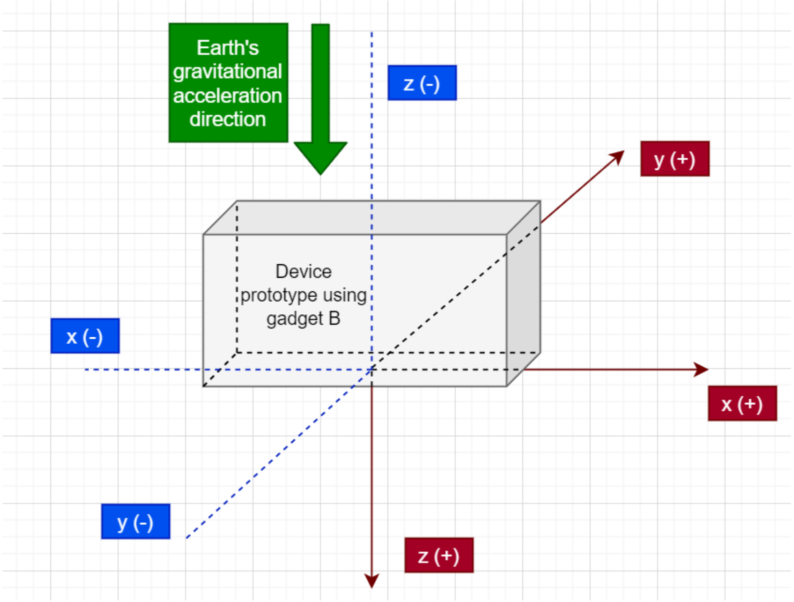
Earth's gravitational acceleration direction
z (-)
y (+)
Device prototype using gadget B
x (-)
x (+)
y (-)
z (+)

Figure 21. Gadget B with BLE GATT functionality orientation.

Below in Figure 22 the accelerometer values were not filtered, the gyroscope values were filtered with low pass 3 dB BW 151.8 Hz filter. Accelerometer values in g are under the “Accelerometer” title and gyroscope values in deg/s are under the “Gyroscope” title. It can be noted that the accelerometer values match the results from Arduino UART and BLE UART screens when the gadget B was tested with similar test settings.

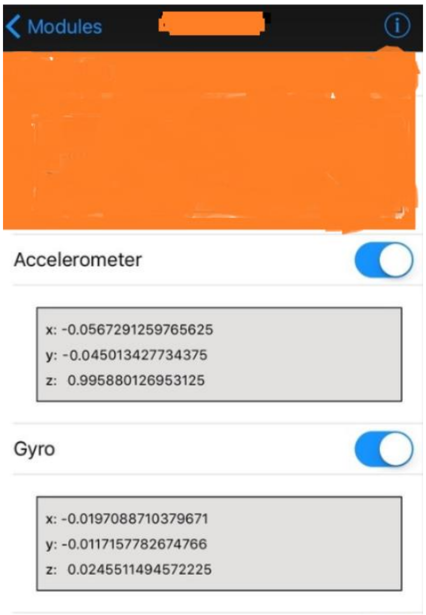

[redacted]

[redacted]

Accelerometer

```
x: -0.0567291259765625
y: -0.045013427734375
z:  0.995880126953125
```

Gyro

```
x: -0.0197088710379671
y: -0.0117157782674766
z:  0.0245511494572225
```

Figure 22. BLE GATT gadget B Accelerometer and Gyroscope values.

As a result, gadget B’s gyroscope and accelerometer board’s accelerometer were added in the final version of the device prototype, because they both had the largest ranges among other breakout boards. The final device prototype used BLE GATT to send the data to a mobile phone. Low pass filter 3 dB BW of 151.8 Hz filtered the gyroscope sensor data and no filtering was applied to the accelerometer sensor data because the accelerometer data was stable and did not fluctuate very drastically. Since the offsets in gyroscope and accelerometer were minor, the calibration was not necessary.

7 Conclusion

The device prototype was successfully implemented using Arduino IDE tools for real-time applications. The device was able to measure linear acceleration and rotational velocity which were the main elements of HITS. Therefore, the device prototype passed the general requirements for collecting the head impact data in accordance with HITS. The impact data was successfully sent over the BLE protocol to the mobile phone. In addition, the device prototype proved to use little power and it proved to have light and compact design. The device prototype was approved by the MDS Finland company.

One of the possible limitations in the future could be the detection of false-positive head impacts like it was mentioned in empirical examples chapter study. In order to improve the accuracy, similar solution as in the empirical examples chapter study- video recording head impact verification method could be implemented. SPI communication protocol can be used instead of I2C to prolong battery life and to increase the speed of transmission. The processor implementing chip could be changed to a chip that does not use on-chip debugger to cut manufacturing costs.

Future development plan includes rotational velocity to rotational acceleration conversion, head impact data cloud storage configuration, EEPROM data storage configuration, and video recording method. EEPROM memory will store data when the wireless communication connection is lost and is to hand it over wireless communication when the connection is restored. The results of the development will later be used for measuring head impacts in hockey players. Hockey player’s potential to obtain head injury will be calculated by AI program which would be observing and learning the behavior of medical professionals analyzing the head impacts. Next GCC and Segger IDEs compilers would replace Arduino IDE, because Segger IDE is more flexible and creates more power-efficient applications than Arduino IDE. In addition, nRF51 SDK would be used in order to make the development process more flexible, because it has many useful software tools and libraries.

References

[1] UPMC [Online]. Concussion and Loss of Consciousness. Accessed on 12.04.2020. URL: https://share.upmc.com/2015/04/concussion-and-loss-of-consciousness/

[2] MDS Finland's webpage [Online]. Accessed on 23.04.2020. URL: https://www.mdsfinland.com/main/

[3] Mayo Clinic [Online]. Concussion. Accessed on 08.04.2020. URL: https://www.mayoclinic.org/diseases-conditions/concussion/symptoms-causes/syc-20355594

[4] OrthoInfo [Online]. Sports Concussion. Accessed on 08.04.2020. URL: https://orthoinfo.aaos.org/en/diseases--conditions/sports-concussion

[5] UPMC statistics [Online]. Accessed on 23.04.2020. URL: https://www.upmc.com/services/sports-medicine/services/concussion/facts-statistics

[6] TBI [Online]. Accessed on 23.04.2020. URL: https://mayfieldclinic.com/pe-tbi.htm

[7] Air Force Center of Excellence for Medical Multimedia [Online]. Mechanisms of TBI. URL: https://tbi.cemmlibrary.org/Mild-TBI-Concussion/Mechanisms-of-TBI

[8] Jeffrey T. Barth, Jason R. Freeman, Donna K. Broshek, and Robert N. Varney [Online]. Acceleration-Deceleration Sport-Related Concussion: The Gravity of It All. Accessed on 08.04.2020. URL: https://www.ncbi.nlm.nih.gov/pmc/articles/PMC155415/

[9] Khan Academy [Online]. What is Torque? Accessed on 27.05.2020. URL: https://www.khanacademy.org/science/physics/torque-angular-momentum/torque-tutorial/a/torque

[10] Systematic review [Online]. Accessed on 08.04.2020. URL: https://www.ncbi.nlm.nih.gov/pmc/articles/PMC5384819/

[11] Washington State University [Online]. Inaccuracies in head impact sensors. Accessed on 23.04.2020. URL: https://www.sciencedaily.com/releases/2015/08/150824130822.htm

[12] Calvin Kuo, Lyndia Wu, Jesus Loza, Daniel Senif, Scott C. Anderson, David B. Camarillo [Online]. Comparison of video-based and sensor-based head impact exposure. Accessed on 01.03.2020. URL: https://journals.plos.org/plosone/article?id=10.1371/journal.pone.0199238

[13] Sportsknowhow [Online]. Field hockey field dimensions. Accessed on 23.04.2020. URL: https://sportsknowhow.com/field-hockey/dimensions/field-hockey-dimensions.html

[14] Gebreyesus, Yonas Yosef [Online]. Hardware Design for Head Impact Assessment in Contact Sports. Accessed on 23.04.2020. URL: https://www.theseus.fi/handle/10024/173488

[15] Siliconlabs. Which ARM Cortex Core Is Right for Your Application? Published on 27.03.2020.

[16] Bluetooth [Online]. At core of everything Bluetooth. Accessed on 23.04.2020. URL: https://www.bluetooth.com/specifications/bluetooth-core-specification/

[17] Sergio Silva, Antonio Valente, Antonio Valente, Salviano Soares, A. Paulo Moreira, A. Paulo Moreira [Online]. Coexistence and Interference Tests on a Bluetooth Low Energy Front-End. Accessed on 23.04.2020. URL: https://www.researchgate.net/publication/265602069c_Coexistence_and_Interference_Tests_on_a_Bluetooth_Low_Energy_Front-End

[18] Tornbjorn Ovrebekk [Online]. The Importance of Average Power Consumption to Battery Life. Accessed on 23.04.2020. URL: https://blog.nordicsemi.com/getconnected/the-importance-of-average-power-consumption-to-battery-life

[19] Svein Kleiven [Online]. Why Most Traumatic Brain Injuries are Not Caused by Linear Acceleration but Skull Fractures are? Accessed on 23.04.2020. URL: https://www.ncbi.nlm.nih.gov/pmc/articles/PMC4090913/

[20] Yida [Online]. UART vs I2C vs SPI – Communication Protocols and Uses. Accessed on 23.04.2020. URL: https://www.seeedstudio.com/blog/2019/09/25/uart-vs-i2c-vs-spi-communication-protocols-and-uses/

[21] Paul Romano [Online]. Arduino Development Kits: Advantages and Features. Accessed on 23.04.2020. URL: https://www.semiconductorstore.com/blog/2014/Arduino-Development-Kits-Advantages-and-Features/811/

[22] Arduino [Online]. What is Arduino? Accessed on 23.04.2020. URL: https://www.arduino.cc/en/guide/introduction

[23] How to mechatronics [Online]. How I2C Communication Works and How To Use It with Arduino. Accessed on 26.05.2020. URL: https://www.youtube.com/watch?v=6IAkYpmA1DQ

[24] Nordic semiconductor devzone [Online]. Bluetooth low energy Characteristics, a beginner's tutorial. Accessed on 1.05.2020. URL: https://devzone.nordicsemi.com/nordic/short-range-guides/b/bluetooth-low-energy/posts/ble-characteristics-a-beginners-tutorial

[25] Leanne Young, Gregory T. Rule, Robert T. Bocchieri, Timothy J. Walilko, Jennie M. Burns and Geoffrey Ling [Online]. When physics meets biology: low and high-velocity penetration, blunt impact, and blast injuries to the brain. Accessed on 23.04.2020. URL: https://www.frontiersin.org/articles/10.3389/fneur.2015.00089/full

[26] SAE Dummy Testing Equipment Subcommittee [Online]. Sign conversion

for vehicle crash testing. Accessed on 25.05.2020. URL: https://law.resource.org/pub/us/cfr/ibr/005/sae.j1733.1994.html

[27] Anna Oeur, Clara Karten, T, Blaine Hoshizaki. Impact frequency validation of the head impact sensor technology for use in sport. Published on: 22.07.2016.